Analyst

ROYAL SOCIETY OF CHEMISTRY

CRITICAL REVIEW

View Article Online
View Journal | View Issue

Cite this: *Analyst*, 2022, **147**, 4674

Recent advances in antibiotic resistance diagnosis using SERS: focus on the "*Big 5*" challenges

Waleed A. Hassanain, [a] Christopher L. Johnson,[b] Karen Faulds, *[a] Duncan Graham *[a] and Neil Keegan*[b]

Antibiotic resistant bacteria constitute a global health threat. It is essential for healthcare professionals to prescribe the correct dose of an effective antibiotic to mitigate the bacterial infection in a timely manner to improve the therapeutic outcomes to the patient and prevent the dissemination of antibiotic resistance. To achieve this, there is a need to implement a rapid and ultra-sensitive clinical diagnosis to identify resistant bacterial strains and monitor the effect of antibiotics. In this review, we highlight the use of surface enhanced Raman scattering (SERS) as a powerful diagnostic technique for bacterial detection and evaluation. Initially, this is viewed through a lens covering why SERS can surpass other traditional techniques for bacterial diagnosis. This is followed by different SERS substrates design, detection strategies that have been used for various bacterial biomarkers, how SERS can be combined with other diagnostic platforms to improve its performance towards the bacterial detection and the application of SERS for antibiotic resistance diagnosis. Finally, the recent progress in SERS detection methods in the last decade for the "*Big 5*" antibiotic resistant challenges as demonstrators of public health major threats is reviewed, namely: *Methicillin-resistant Staphylococcus aureus* (*MRSA*), *Carbapenem-resistant Enterobacteriaceae* (*CRE*)/*Extended-spectrum beta-lactamases* (*ESBLs*), *Mycobacterium tuberculosis* (*TB*), *Vancomycin-resistant Enterococcus* (*VRE*) and *Neisseria Gonorrhoea* (*NG*). This review provides a comprehensive view of the current state of the art with regard to using SERS for assessing antibiotic resistance with a future outlook on where the field go head in the coming years.

Received 24th April 2022,
Accepted 10th September 2022

DOI: 10.1039/d2an00703g

rsc.li/analyst

[a]*Department of Pure and Applied Chemistry, Technology and Innovation Centre, University of Strathclyde, Glasgow, G1 1RD, UK. E-mail: duncan.graham@strath.ac.uk, karen.faulds@strath.ac.uk*
[b]*Translational and Clinical Research Institute, Newcastle University, Newcastle-Upon-Tyne, NE2 4HH, UK. E-mail: neil.keegan@ncl.ac.uk*

1. Introduction

Antibiotic resistance is one of the major global concerns to the public health. It occurs when bacteria develop resistance against the antibiotics designed to kill them, which enable the

Waleed A. Hassanain

Waleed Hassanain is a Postdoctoral Research Associate in the Department of Pure and Applied Chemistry at the University of Strathclyde. In 2019, he received his PhD degree in Analytical Chemistry from Queensland University of Technology, Australia. His PhD project was related to developing nanoscale platforms for the isolation and ultra-trace detection of bioactive molecules. His current research focuses on developing ultra-sensitive point of care nanosensing immunoassay for the DNA signature of anti-microbial resistant bacteria using surface enhanced Raman scattering (SERS) technique.

Christopher L. Johnson

Christopher L. Johnson received his PhD in 2007 from the Institute of Cell and Molecular Biosciences, Newcastle University, UK. He is presently a Researcher Co-Investigator at Newcastle University, UK. His current research focuses on the use of isothermal amplification platforms for the rapid detection of infectious organisms as well as the development of capture reagents against novel bacterial biomarkers.

bacteria to survive and grow. Resistance can emerge as a result of mutation or direct transfer of genes encoding a resistance mechanism by conjugation, transformation or transduction.[1] These genetic material, including antibiotic resistance genes, can spread easily between bacteria even those of unrelated species.[1] The main cause of antibiotic resistance is the excessive and inadequate use of antibiotics, which has led to an ever increasing prevalence of resistance genes in bacterial strains, thus increasing the treatment failure and decreasing the available antibiotic regimens. The lack of effective antibiotics can increase the severity of common infections, as well as the morbidity and mortality rates between patients. Globally, antibiotic resistance is responsible for more than 500 000 deaths every year with 40% involving infant deaths.[2] In addition, antibiotic resistance has severe adverse effects on healthcare costs, in term of prolonged treatment, longer hospitalisation and greater risk from the spread of infection. In a recent collaborative CDC study, the estimated cost to treat infections caused by six multidrug-resistant pathogens in the USA alone can be more than $4.6 billion annually.[3] Therefore, urgent action is required to mitigate and combat the emergence and spread of the antibiotic resistance threat. The mitigation measures include, but are not limited to, develop new classes of antibiotic, control the use of antibiotics, improve infection control measures, strengthen detection and develop rapid clinical diagnostics for antibiotic resistant bacteria.

The ability to accurately measure the burden of antibiotic resistance on populations is a critical and challenging task which is necessary in order to define priority areas for intervention. A novel metric to estimate this burden is disability-adjusted life-years (DALYs).[4] Using this composite health measure of DALYs per 100 000 people, it has been estimated that the antibiotic resistance lead to 170 DALYs per 100 000 people in Europe with about 75% of the total burden of infections associated with health care.[4] Based on this estimate of DALYs for antibiotic resistant bacteria, the greatest challenges currently in Europe are: [1] *Carbapenem-resistant Enterobacteriaceae* (*CRE*)/*Extended-spectrum beta-lactamases* (*ESBL*) produced by Gram-negative bacteria, [2] *Methicillin-resistant Staphylococcus aureus* (*MRSA*), [3] *Vancomycin-resistant Enterococcus* (*VRE*) and [4] *Mycobacterium tuberculosis* (*TB*).[4,5] Although there is no estimate of the burden of *Neisseria Gonorrhoea* (*NG*) by DALYs in Europe, it is known to be a huge problem with rapidly increasing rates of resistance.[6] Based on this information, *Neisseria Gonorrhoea* should be considered as one of the "*Big 5*" antibiotic resistance challenges.

The leading challenges in the clinical diagnosis of antibiotic resistance and its causative pathogens are the speed and sensitivity of the detection methodology.[7] The rapid and early identification of the microbial pathogens allows for the quick and appropriate medical intervention, thus reducing the case fatality rate and healthcare costs associated with a bacterial infection. At the same time, therapeutic drug monitoring and bacterial susceptibility testing for the antibiotics used are the cornerstone to understand and improve their therapeutic effect. This also requires the use of sensitive techniques that can rapidly evaluate the relationship between antibiotic dosage concentration and the clinical response during different stages of the treatment protocol. Accordingly, there is a continuous demand within the molecular diagnostics market for rapid, sensitive and cost-effective detection techniques that can be miniaturized for the reliable screening of pathogenic bacterial biomarkers that indicate the presence of antibiotic resistant bacteria, as well as to estimate the antibiotic susceptibility of the bacteria in biological specimens.

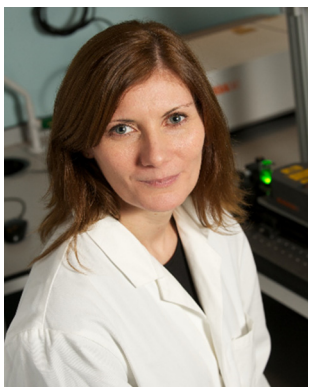

Karen Faulds

Karen Faulds is a Distinguished Professor at the University of Strathclyde and an expert in the development of SERS and Raman techniques for novel analytical detection strategies, in particular multiplexed bioanalytical applications. She has published over 150 publications and her Groups' research has been recognised through multiple awards. She is a Fellow of the Royal Society of Chemistry (RSC), Society for Applied Spectroscopy and Royal Society of Edinburgh. She is Chair of the Infrared and Raman Discussion Group (IRDG), an elected member of the RSC Analytical Division Council and the Federation of Analytical Chemistry and Spectroscopy Societies (FACSS) Governing Board. She is an Associate Editor for Analyst and serves on the editorial board of RSC Advances and Analyst and advisory board for Chemical Society Reviews.

Duncan Graham

Duncan Graham is a Distinguished Professor and Associate Principal and Executive Dean of Science at the University of Strathclyde. He served as Editor in Chief of the RSC journal Analyst and was president of the analytical division of the RSC (2017–2020). He is currently a trustee of and chair of the Publishing Board for the RSC (2020–2024). His scientific interests are in using synthetic chemistry to produce sensors that respond to specific biological species or events as measured by Raman spectroscopy or SERS and collaborating with scientists from different disciplines to exploit these approaches.

Apart from the traditional bacterial culture methods, various methods have been described for the sensitive detection of pathogenic bacterial biomarkers, such as: Nucleic acid amplification tests (NAATs),[8] mass spectrometry (MS),[9] enzyme linked immunosorbent assay (ELISA),[7] and the use of electrochemical sensors.[10] NAATs as polymerase chain reaction (PCR) test, are growth-free methods that offer fast results with a reasonable sensitivity and specificity. However, inability to distinguish viable from nonviable bacterial cells, high cost of the analysis and the need for experienced laboratory technicians are considered as NAATs limitations.[11] MS techniques as matrix-assisted laser desorption/ionization (MALDI) and electrospray ionization (ESI) are important tools for separation, classification and identification of bacteria and other microorganisms in one matrix.[12] These methods can easily distinguish bacteria on the genus, species and, sometimes, subspecies level. However, MS suffers from being an expensive technique and requires extensive sample preparation procedures by trained operators which increase the detection turnaround time.[13] ELISA is also commonly used in pathology laboratories for bacterial biomarker detection. Generally, it has a good specificity and can handle large number of samples with a reasonable sensitivity using automated equipment.[7] Like MS, ELISA requires tedious and laborious procedures for the preparation of the assay. In addition, a relatively high sample volume is required otherwise there will be a high possibility of false positive or negative results.[14] Electrochemical sensing techniques have attracted considerable attention as an analytical tool for the detection of bacterial biomarkers. The use of nanomaterials, such as: metallic nanostructures, metal oxide semiconductors and carbon nanotubes/nanosheets, in the manufacture of the electrochemical sensors improved their conductivity and sensitivity.[15–17] However, the measurements reproducibility in complex matrices is still challenging for reliable sensing. The potential interfering species, such as organic/inorganic contaminants and other biomolecules, limit the lifetime and sensitivity of the sensors, which in turn affect the reliability of the read out.[18] Therefore, it is still highly desirable for a rapid and sensitive point of care (POC) bacterial diagnostic technique that can meet the standards obtained in pathology laboratories.

Surface enhanced Raman spectroscopy (SERS), a highly sensitive variation of Raman spectroscopy, is a suitable alternative technique. Since its discovery more than four decades ago, SERS has been successfully used in different fields, such as: environmental screening,[19] antimicrobial resistance detection,[20] food and pharmaceuticals analysis.[21,22] SERS is a powerful analytical technique that can be used for the ultrasensitive qualitative interpretation and quantitative detection of bacterial biomarkers which can give insight into the bacterial infection severity.[23] In addition to its eminent sensitivity, SERS offers good specificity and strong multiplexing ability. Advances in the manufacturing technology enabled the development of user-friendly and cost-effective portable Raman spectrometers that can move SERS measurements from localized laboratories to POC and infield analysis. This facilitates acquisition of fast test results and minimising sample backlogs. Additionally, it can reduce the biological risks associated with the transportation of infectious biological samples to centralised laboratories, especially during an outbreak of highly contagious diseases like the recent Covid-19 coronavirus. The distinct advantages of SERS for the detection of bacterial biomarkers over other analytical techniques include: [1] its ability to achieve ultra-sensitive detection of the analyte.[24] Therefore, it can be used for the early diagnosis of bacterial infection when the trace levels of bacterial biomarkers still cannot be detected by other techniques. [2] Its multiplexing capability, as SERS can be used for analysis of multiple components in one matrix, with minimal sample pre-treatment steps. Unlike fluorescence, SERS has narrow spectral Raman bands that allows for the easily spectral separation between different peaks corresponding to multiple components in one sample matrix.[24] [3] Its capacity to provide rich spectral information for the molecular structure of the antigen as a fingerprint tool which can define specific diseases with minimal sample handling.[25] Furthermore, SERS can detect the antigens in aqueous matrix, as water has a weak Raman scattering due to its small Raman cross-section.[26] This facilitates the direct detection of antigens in biological fluids. Due to these advantages, SERS has been extensively demonstrated in molecular diagnostics research over the last decade as a proof-of-concept tool for *in vitro* and *in vivo* diagnosis of different diseases in biofluids, cells or biopsy samples.[24,27]

Despite its high sensitivity, SERS has some drawbacks, such as: [1] the spontaneous fluorescence radiation can mask or quench the SERS signals and affect the sensitivity of the detection.[28] This can be minimised by using a suitable modification technology for the nanostructured surface.[29] [2] The lack of

Neil Keegan

Neil Keegan is a Senior Lecturer at Newcastle University in the Translational and Clinical Research Institute. He specialises in medical biotechnology, particularly biosensors and biological sensor systems. He is currently a Director of the Newcastle University Centre of Research Excellence (NUCoRE) in Biomedical Engineering and on the steering group for the Molecular Mechanisms of life research theme at Newcastle University. He has a background in protein engineering and the design of hybrid surfaces for bio-molecule immobilisation, having held an MRC-sponsored PhD studentship in Bionanotechnology. The use of recognition molecules at interfaces led him towards biosensor and general diagnostic development programs with a current interest in infectious disease diagnostics and antimicrobial resistance.

selectivity.[30,31] SERS cannot be used independently for the selective detection of an antigen when it presents with other interfering molecules in a mixture. This can be solved by using selective antigen-recognition molecules, such as antibodies and aptamers, or by combining SERS with another separation technique, such as HPLC prior to the SERS measurements.[32,33] [3] SERS variability, in term of signal intensity.[34] However, due to advances in the design and synthesis of highly reproducible SERS substrates, SERS now is used successfully for the reproducible quantitative measurements of different targets in different matrices.[35] Moreover, the recent large inter-laboratory studies set the good analytical practice to improve SERS results reproducibility between laboratories.[36,37] Therefore, due to these unique characteristics, SERS can be considered as a strong promising alternative for the traditional bacterial detection methods for real life samples.[38]

In this review, the use of SERS for the detection of bacteria is discussed. This will be followed by the application of SERS in the diagnosis of antibiotic resistance based on the identification of the resistant and non-resistant bacterial isolates, as well as the determination of antibiotic susceptibility of the bacteria. Finally, we highlight the recent advance in SERS methods for the detection of the "*Big 5*" antibiotic resistant challenges in the last 10 years.

2. SERS for bacterial detection

2.1. Mechanism of SERS

The SERS effect was first reported in 1974 by Fleischmann and co-workers.[39] Later in 1977, Jeanmaire and Van Duyne[40] reported a significant Raman signal enhancement that was attributed to the adsorption of molecules onto a roughened noble metal surface as metallic nanostructures. Although the exact explanation of SERS theory is still a matter of debate in the literature, it is widely accepted now that SERS enhancement is attributed to the combined effect of electromagnetic and chemical enhancements.[41] The electromagnetic enhancement is the dominant contributor for the SERS effect. It arises from the localized surface plasmon resonance (LSPR) close to the nanostructured noble metals surface, such as gold and silver.[42] Highly localized regions of amplified electromagnetic fields caused by LSPR are called "hot spots", which usually occurs in the gaps, crevices, or sharp vertices of the nanostructures (Fig. 1).[43] When the analyte is trapped within or near the hot spot areas, its SERS signal become greatly enhanced by laser excitation with an enhancement factor of 10^6–10^8 compared to conventional Raman signal. Compared to the electromagnetic enhancement, the chemical enhancement can contribute approximately from 10^2 to 10^3 orders of magnitude to the overall SERS signal enhancement.[41] This enhancement is attributed to the electron transfer between the analyte molecule and the surface of the nanostructure when the incident light matches the electron transfer energy. This will lead to a change in the molecular polarization and enhance the Raman signal of the analyte.[43]

Considering SERS merits of ultrahigh sensitivity down to single level of molecule,[44] multiplex detection capability and potential for on-site applications, SERS-based methods have attracted increasing attention as a reliable tool for the specific detection of different pathogenic bacterial biomarkers (nucleic acids, proteins and cell metabolites).[45] For example, a recent study demonstrated the use of a SERS-lateral flow platform for the ultra-sensitive duplex quantification of clinically relevant pathogenic bacterial biomarkers of *Clostridium difficile* infection at low cost within a short time. Combined with the simple manual operation and small sample volume, the method provided a potential application in POC.[23]

2.2. SERS substrates for bacterial detection

In order to acquire a strong SERS signal for bacterial detection, a sensitive SERS substrate should be used as a platform for the measurements. The antigen must be adsorbed in close proximity to the enhancing metal surface. The magnitude of the enhancement effect is strongly influenced by the nanostructures size, shape, and surface structure, as well as the antigen proximity to the SERS substrate. The ideal SERS substrate should be [1] highly stable, [2] offer strong signal enhancement, [3] provide reproducible and uniform response and [4] can be fabricated easily using cost-effective methods.

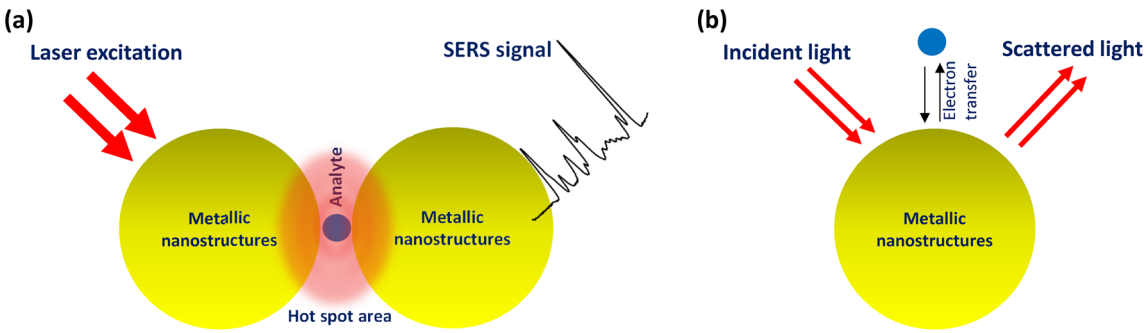

Fig. 1 Mechanisms of SERS effect through (a) electromagnetic enhancement of SERS, where analyte is trapped in the hot spot area formed between two adjacent SERS active metallic nanostructures, and (b) electron transfer between SERS active metallic nanostructure and analyte, resulting in chemical enhancement of SERS.

Generally, SERS substrates for bacterial detection can be classified into colloidal and solid-based nanostructure substrates. Although SERS signal reproducibility problems arise from these substrates, the colloidal nanostructured substrates can be easily synthesised and functionalised by multiple facile and low-cost chemical methods.[46–48] The aggregation of colloidal plasmonic nanostructures causes their surface plasmon to couple and leads to a strong local electromagnetic field enhancement.[46,49] In addition, the 3D geometry of colloidal nanostructures allows for their efficient interaction with the antigen, thus increasing the SERS signal enhancement.[47,50] For example, spermine stabilised silver nanoparticles (AgNPs) were demonstrated as a colloidal SERS substrate for the simple and direct detection of DNA duplexes.[51] The positively charged AgNPs allowed for controlled aggregation, which provided the required hot spots for SERS, without the need of using aggregating agent as the DNA itself induced the aggregation of NPs and formation of small stable clusters *via* electrostatic interactions. Due to the small amount of DNA sample required, the analysis provided significant information on the DNA in its native state without the necessity of pre-amplification methods. Similarly, the colloidal nanoparticles can be physically adsorbed onto the surface of bacterial cell to enable SERS measurements.[52] For example, Kahraman *et al.* developed a layer-by-layer coating method for the detection of *Escherichia coli* (*E. coli*) and *Staphylococcus cohnii* (*S. cohnii*) using AgNPs and/or AuNPs.[53] The bacteria were initially coated with the positively charged polymer poly(allylamine hydrochloride). The negatively charged NPs were then electrostatically adsorbed on the bacterial cell surface and enabled direct characterisation by SERS.

On the other hand, a solid-based nanostructured substrate provides a higher signal enhancement with better reproducibility and uniformity than the colloidal substrates.[54] It is fabricated *via* two main approaches, either by immobilising nanostructures onto a solid support or by fabricating nanostructures directly onto solid substrates by lithographic techniques.[55] The first approach utilises wet chemistry methods to synthesise colloidal metallic nanostructures that can then be deposited onto different solid platforms, such as glass or paper, *via* specific immobilisation techniques.[55] This approach could result in non-patterned substrates like paper-SERS substrate, where the plasmonic nanostructures are randomly distributed onto the paper surface. Despite being simple and inexpensive, this approach requires elaborate design and careful operation to maintain substrate reproducibility and minimise batch-to-batch variation. For example, Fan *et al.*[56] developed a graphene oxide attached to popcorn-shaped AuNPs as a hybrid SERS probe for the ultrasensitive label-free sensing of *HIV-1* DNA (femto-molar level) and *MRSA* (10 CFU mL^{-1}) (Fig. 2). Although the obtained SERS spectra from DNA using different substrate batches indicated good SERS reproducibility, the method did not report the relative standard deviation values between the measurements to express the SERS signal reproducibility in a quantitative way. A similar substrate design was also demonstrated for the simultaneous label-free SERS identification and eradication of *MRSA*. The substrate composed of chitosan conjugated plasmonic AuNPs attached to a 3D hybrid graphene oxide membrane.[57]

The second approach utilises lithographic methods, such as: focused ion beam milling and electron-beam lithography, where the nanostructures are directly fabricated onto a solid support surface such as silicon wafer. This approach can precisely control the size and shape of the nanostructures and produce highly patterned and uniform nanostructure assemblies onto the surface of the solid support, and thereby enabling a high reproducibility for the SERS measurements. However, it requires expensive instrumentation and trained operators.[58] For example, Wu *et al.* developed vancomycin functionalised Ag nanorod (AgNR) array substrates for the

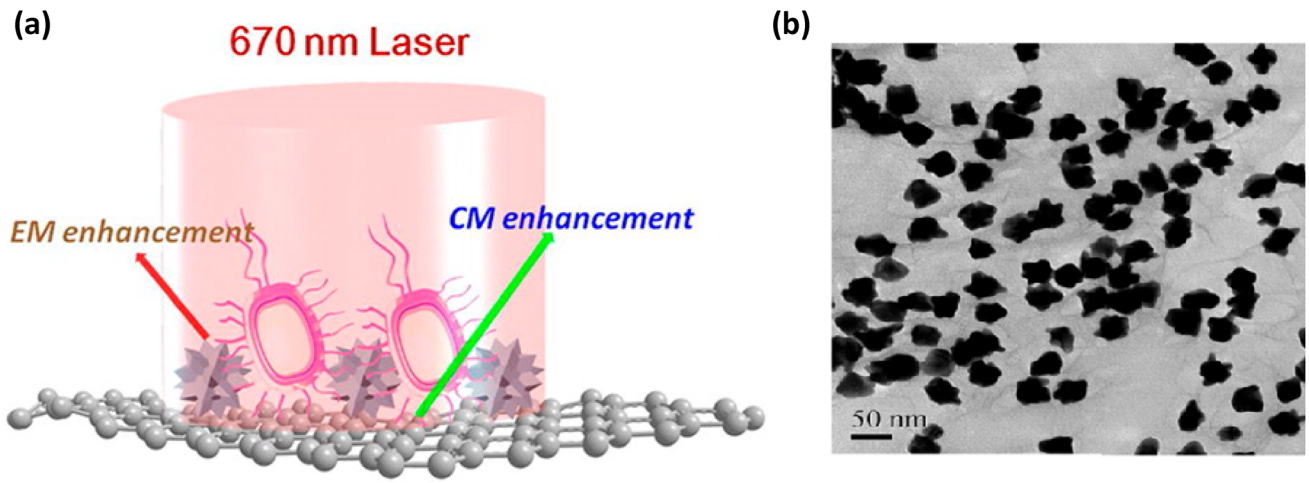

Fig. 2 (a) Schematic representation shows the hybrid graphene oxide-based SERS probe for tuning electromagnetic and chemical enhancement simultaneously to detect *MRSA*. (b) TEM image showing the morphology of the hybrid graphene oxide, where graphene oxide has been attached to nanopopcorn. The image is reprinted from Fan *et al.*,[56] Copyright (2013), with permission from American Chemical Society.

detection of six foodborne pathogenic bacteria in mung bean sprouts samples. The AgNR array substrate was formed by the deposition of AgNRs onto a glass slide by the oblique angle deposition technique (OAD) using a custom-designed electron beam/sputtering evaporation system. The substrate was then immersed in vancomycin solution overnight for complete functionalisation before incubating with bacterial samples. With the aid of principal component analysis (PCA), the reported limit of detection (LOD) was 10^3 CFU g^{-1} of mung bean sprouts. The developed substrate demonstrated a SERS enhancement factor $>10^8$ and a batch variability <15%.[59] For extended information on the recent interesting advances in SERS substrate designs and applications, the reader could refer to some excellent reviews such as Langer *et al.*,[35] Wang *et al.*[60] and Zong *et al.*[61]

2.3. SERS strategies for bacterial detection

Bacterial SERS detection can be either label-free (intrinsic) or label-based (extrinsic). The label-free SERS involves mixing the bacterial sample directly with metallic nanostructures in a solution or forming a thin film onto a solid SERS substrate for bacterial attachment, resulting in SERS signals for the bacterial sample itself.[62] This technique takes the full advantage of the fingerprint information of SERS, as it provides detailed structural information for the bacterial sample. For example, a label-free SERS method was demonstrated by Yang *et al.* for the detection of *E. coli*.[63] The bacterial sample was mixed directly with AgNPs under certain optimised incubation conditions (shaking speed, time and temperature) that delivered the strongest SERS enhancement. The method was used successfully to discriminate between three strains of the bacteria using statistical analysis. The reported limit of detection that could be detected by SERS mapping was 1×10^5 cell per mL.

Label-based SERS involves the functionalisation of the nanostructures with a specific target-recognition molecule (*i.e.*, antibody, aptamer, enzyme, *etc.*) and a Raman label to form a SERS nanotag. The SERS nanotag will selectively capture the target antigen from complex matrices and produce strong and characteristic Raman signal for the label that indirectly indicates the presence and/or determines the concentration of the bacteria in the sample.[38] Duan *et al.* reported an indirect SERS-based aptasensor for the determination of *Salmonella typhimurium* (*S. typhimurium*) in milk.[64] They used Au@Ag core/shell NPs functionalised with target-selective capture aptamer (Au@Ag-apt 1) and X-rhodamine (Raman label) conjugated to the same aptamer (ROX-apt 2). As per Fig. 3, *S. typhimurium* interacted selectively with the aptamers to form Au@Ag-apt 1-target-apt 2-ROX sandwich-like complex. By monitoring the SERS signal of the Raman label at 1638 cm^{-1}, a linear calibration curve was obtained in the range of 15 to 1.5×10^6 CFU mL^{-1} with a limit of detection of 15 CFU mL^{-1}.

Compared to label-based SERS detection, the label-free SERS procedure is simpler and more straight forward. However, it requires a highly efficient SERS substrate and strong nanostructure-analyte binding for strong SERS signal and reproducible results. The label-based SERS strategy can increase the sensitivity of the detection limits and enable a multiplex detection of pathogenic bacteria through the use of multiple target-recognition molecules with different Raman labels. However, it is not detecting the target bacterial sample itself, it depicts the SERS spectrum of the Raman label.

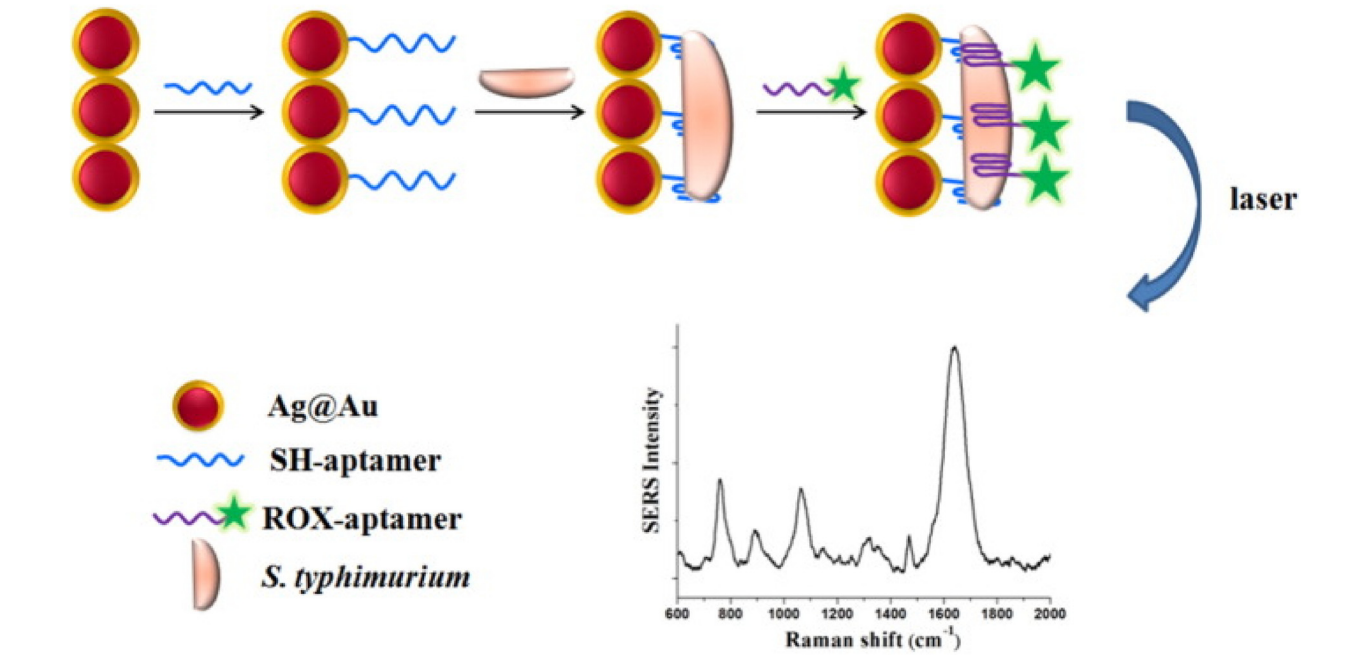

Fig. 3 Schematic illustration of SERS-based aptasensor for quantification of S. *typhimurium*. The image is reprinted from Duan *et al.*,[64] Copyright (2016), with permission from Elsevier.

Therefore, the rich biological information of the bacterial sample will be lost.

Beside label-free and labelled SERS detection, SERS bacterial imaging and mapping was used to deeply understand how bacteria can resist or inactivate the antibiotics action which has crucial importance in antibiotic resistance assessment. The chemical imaging and mapping of pathogenic bacteria can yield significant insight into a wide range of properties including the infectious bacterial biomarker distribution inside the sample. Due to the rich spectral vibrational information that SERS can offer, SERS was used as unique and non-destructive technique for bacterial chemical imaging.[65–67] For example, Ag dendrites were employed for rapid chemical mapping of pure and mixed samples of *Salmonella enterica* and *E. coli*.[68] The dendrites were mixed with the bacterial suspensions, dried and the SERS imaging was recorded within 24 min using peak intensity at 1332 cm^{-1}. SERS maps were analysed with PCA to determine the concentrations and the distribution of the two bacterial species simultaneously and with other bacterial mixtures. The reported LOD was 10^4 CFU mL^{-1}.

SERS has also been coupled with other diagnostic platforms to improve the SERS efficiency towards bacterial detection. This coupling enhanced the overall performance of SERS detection, in term of speed, robustness and the right diagnosis. Additionally, it promoted SERS to provide a real-time and onsite diagnosis for different bacterial biomarkers. Therefore, rapid action could be taken towards the bacterial infections in a short time instead of just monitoring the patient's general health status or trying to control the infection severity by using inappropriate treatment that can increase the risk of dissemination of antibiotic resistance. Lateral flow assay (LFA), microfluidic and lab-on-a-chip (LoC) devices are among the most common diagnostic platforms that have been integrated with SERS and used in POC applications for the diagnosis of bacterial biomarkers.[45,69] These platforms can satisfy the cost effectiveness and reproducibility needs of the measurements. In addition, they are stable over a long period of time, biocompatible with biological fluids and support multiplexing analysis without sophisticated sample preparation procedures. Therefore, by coupling the advantages of these platforms with the other SERS merits, these combinations are expected to enable the potential shift of SERS measurements from R & D laboratories to practical real-world applications.

SERS based-LFA has attracted increasing attention as an alternative tool for the traditional bacterial detection methods as a sensitive, selective, simple, cheap and user-friendly platform. Choo's group has demonstrated the use of different SERS based-LFA applications for the detection of different pathogenic bacteria.[70] For example, a SERS-based lateral flow immunoassay biosensor was developed for the detection of food poisoning pathogen *Staphylococcal enterotoxin B* (*SEB*) to resolve the low sensitivity issue that associated with conventional LFA strips.[71] For this purpose, hollow Au nanospheres were functionalised with a Raman label and antibody and used as a SERS detection probe that specifically captures and detects the target pathogen. The method was able to detect 0.001 ng mL^{-1} based on the SERS signals measured on the test line. The detection limit was more sensitive by almost three orders of magnitude compared to an ELISA. Recently, the same group reported another SERS-LFA method for the rapid serodiagnosis of *Orientia tsutsugamushi IgG* (scrub typhus biomarker).[72] To assess the clinical feasibility of the proposed assay, the developed platform was tested on 40 clinical sera samples. The results were cross validated against standard indirect immunofluorescence method with a good agreement. The group also reported the use of a portable Raman spectrometer device-under development-that is compatible with the LFA strips. The device dimensions are 16 × 22 × 9.5 cm and contains a slot where the strips can be inserted into for the measurement. In addition, special Raman software was developed for an automated mapping analysis for the test and control lines. Therefore, this method demonstrated a new POC diagnostic platform for the infectious diseases and provided an accurate quantification of clinical samples.

Beside SERS based-LFA, the use of a SERS-microfluidic immunoassay combination was also considered as a potential popular platform for the rapid detection of infectious bacteria in clinical samples.[45,65] The advance in the manufacturing methods of microfluidic devices and the use of microchannels, microvalves, micromixers and micropumps have enabled the development of LoC nanosensors with a smaller footprint and reduced cost. The combination of SERS with LoC in one platform facilitates the performance of all the needed procedures for bacterial immunoassay in one step while maintaining the high resolution and sensitivity for the pathogens' detection. The main advantages of the SERS-LoC approach are: [1] the capability of processing low sample volumes using lower amounts of expensive reagents, [2] short times for analysis, [3] automation, and reduction in human error.[45,65,69] Therefore, several research applications discussed the application of the SERS-LoC combination for different bacterial diagnosis. For example, Catala *et al.* demonstrated online SERS quantification of *Staphylococcus aureus* (*S. aureus*) in different human fluid samples *via* a microfluidic optical device.[73] In this method, labelled AgNPs functionalised with biorecognition elements (antibody and aptamer) were used to selectively accumulate on the bacteria surface in the collection window when the sample is passing through the microfluidic device, thereby increasing the detection sensitivity. The aptamer-labelled AgNPs generated a higher signal intensity compared to the antibody-labelled AgNPs. This was attributed to the higher affinity of the aptamer-labelled AgNPs towards the bacteria, which induced the rapid coating of the bacteria with the AgNPs. The reported LOD was <15 CFU mL^{-1} in biological fluids. Additionally, the use of SERS with microfluidic devices could enable high throughput, multiplexed and ultrasensitive quantification of pathogens from complex sample matrices. Wang *et al.* reported a SERS-microfluidic diagnostic platform for the duplex sensitive detection of *Entamoeba histolytica* antigens EHI_115350 and EHI_182030 simultaneously.[74] The designed platform composed of a gold surface glass chip with multiple channels coated with highly specific nanoyeast single-chain variable fragments (NYscFv) as a cost-effective recognition molecule instead of antibodies. Once

the target antigen was captured, Raman labelled-AuNPs conjugated with antigen-specific polyclonal antibodies were adsorbed on the surface to produce the specific barcode for the antigen detection. The platform enabled a highly selective and sensitive detection of EHI_115350 (1 pg mL^{-1}) and EHI_182030 (10 pg mL^{-1}).

Dielectrophoresis (DEP) was also integrated with SERS-microfluidic platform for the accurate and highly sensitive infield detection of bacteria. It was used for the rapid separation and concentration of cells, bacteria, and DNA from biological samples, where non-uniform electric fields are applied to awake the movement of objects in fluids due to their electrical properties.[38] For example, Cheng *et al.* reported a DEP SERS-microfluidic platform for the detection and concentration of *S. aureus*, *E. coli*, and *Pseudomonas aeruginosa* (*P. aeruginosa*) in human blood sample at clinically relevant concentrations without using any antibody/chemical immobilisation in less than 5 min.[75] As shown in Fig. 4, AC electric field induced electrokinetic forces (ACEK) were applied to separate and concentrate pathogens from blood for on-chip SERS measurements. This strategy would allow an extremely high density of bacteria to aggregate for effective SERS measurements and specific fingerprints to be obtained for pathogenic identification with no contribution from blood components. In another application, Lin *et al.* developed a nanoaggregate embedded beads-DEP-Raman spectroscopy barcode sensing strategy for the on-line multiplex detection of *Salmonella choleraesuis* and *Neisseria lactamica* down to single bacterium level using different bioconjugated SERS nanoprobes in less than 2 hours.[76] This platform was combined with a confocal micro Raman system in a compact setup for *in situ* detection with an integration time of one second. Then, automated spectral analysis was applied to discriminate the objects of interest based on the collected SERS spectra. The results demonstrated a potential compact DEP-SERS portable system for the highly sensitive on-line detection of pathogens at POC.

To sum up, the continuous growth in SERS-based research for bacterial detection is expected to continue with more opportunities for SERS to be used in the clinical diagnosis of real samples with a high efficiency. The advance in SERS detection strategies have significantly improved the bacterial biosensing sensitivity and selectivity, as well as enabling SERS to become a promising tool for POC diagnosis. However, before moving SERS outside research laboratories to real life samples, careful technique standardisation, optimisation and validation are required. In the next section, the application of SERS as a

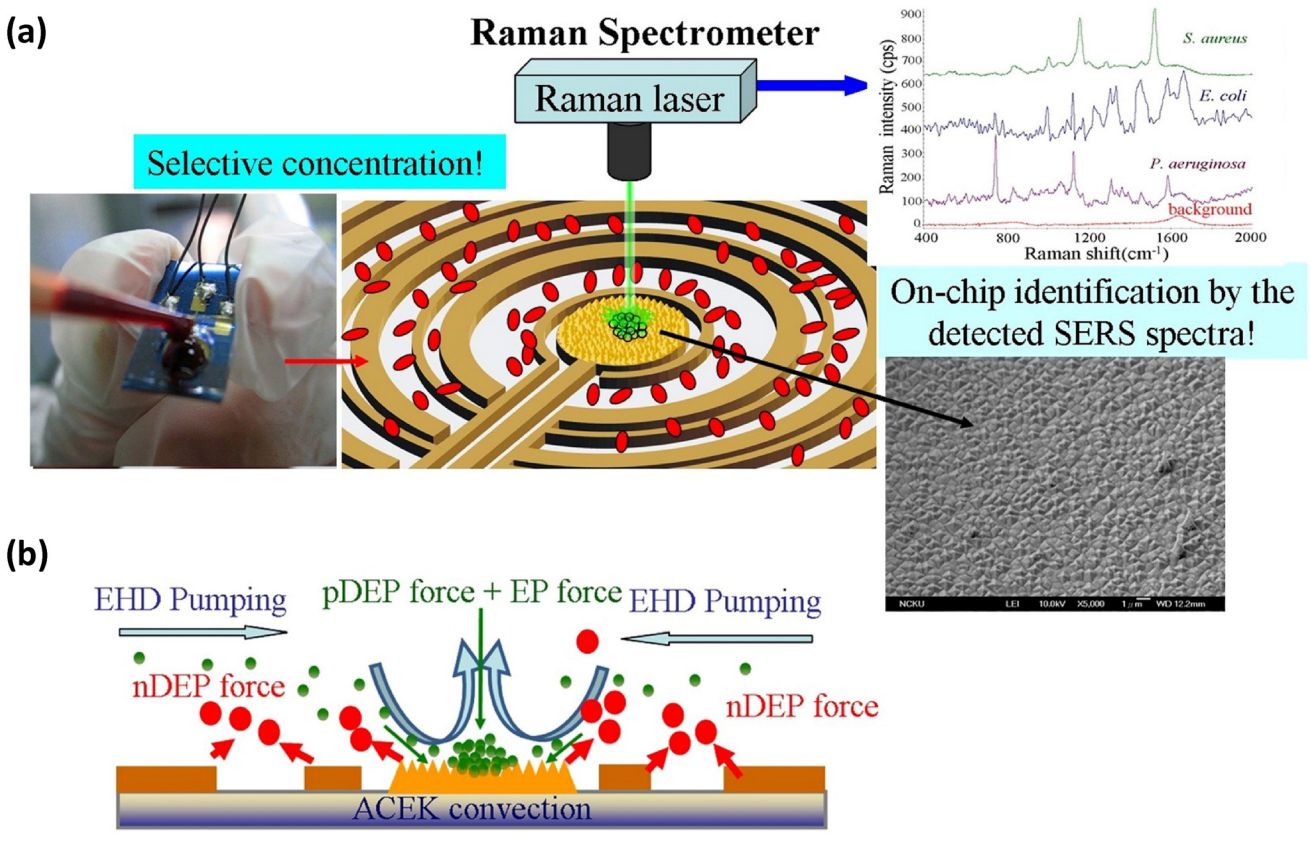

Fig. 4 (a) Experimental setup of the DEP SERS-microfluidic platform. The SEM image shows the roughened Au surface at the centre electrode. AC electric field induced electrophoresis (EP) and electro hydrodynamics (EHD) were used to rapidly concentrate bacteria form human blood. SERS Raman spectroscopy fingerprint of the concentrated bacteria identifies the bacteria. (b) Illustration of the hybrid mechanism of selective concentration over a wide range asymmetric electrode array. The image is reprinted from Cheng *et al.*,[75] Copyright (2013), with permission from Springer Nature.

potential alternative diagnostic tool for bacterial antibiotic resistance based on the discrimination between resistant and non-resistant strains, as well as the determination of bacterial antibiotic susceptibility is highlighted.

3. SERS for antibiotic resistance diagnosis

Molecular diagnostic techniques can be used for the clinical diagnosis of antibiotic resistant bacteria, as well as to generate valuable information about the specific strains/genes responsible for the resistance. However, some critical parameters should be considered when determining the ideal technique, such as: sensitivity, speed and cost.[77]

The use of SERS as a sensitive technique for the rapid and cost-effective detection of antibiotic resistance could generate promising results for clinical applications. As a powerful fingerprint tool, SERS was applied to differentiate between antibiotic resistant and sensitive bacterial strains instead of using traditional time-consuming methods. This is because of the variation in the biochemical compositions of the bacterial cell wall between different strains, which leads to a change in their spectral profile.[43] For example, Cheong *et al.* reported a label-free drop coating SERS method using nano structured aluminosilicate wafer coated with a 50 nm Au film coupled with a multivariate statistical analysis for the rapid discrimination between the clinically relevant quinolone resistant (ST11 and ST15) and control susceptible (ATCC70063) *Klebsiella pneumoniae* (*K. pneumoniae*) strains.[78] The PCA analysis demonstrated a clear difference between the resistant and susceptible strains. Additionally, the statistical analysis discriminated between resistant strain subtypes. In another study, Lu *et al.* reported the first microfluidic-SERS device for the epidemiological monitoring of contagious bacterial infection using samples from China and USA for the differentiation between *Methicillin resistant Staphylococcus aureus* (*MRSA*) and *Methicillin sensitive Staphylococcus aureus* (*MSSA*).[79] Compared to other lengthy techniques, such as PCR, the device managed to perform the differentiation within one hour with the aid of a supervised DFA dendrogram model. A similar microfluidic-SERS platform was applied for the differentiation between different species of mycobacteria including *nontuberculous Mycobacteria* and *Mycobacterium tuberculosis*.[80]

In another application, SERS was also used to demonstrate the difference between the resistant uropathogenic *E. coli* (UTI189, 536) and non-pathogenic *E. coli* (DH5α, TOP10) strains. Firstly, a positively charged glass slide was used to electrostatically collect and immobilise the negatively charged bacteria from the bulk solution within two hours. Then, by using a concentrated AgNPs solution, the SERS spectral fingerprints of both strains were obtained (Fig. 5). The pathogenic strains contain O-antigen of type 6 and 18, which is not present in the non-pathogenic strains. Therefore, clear differences were observed.[81]

The success of SERS in identifying different resistant bacterial strains was extended to perform the detection directly in

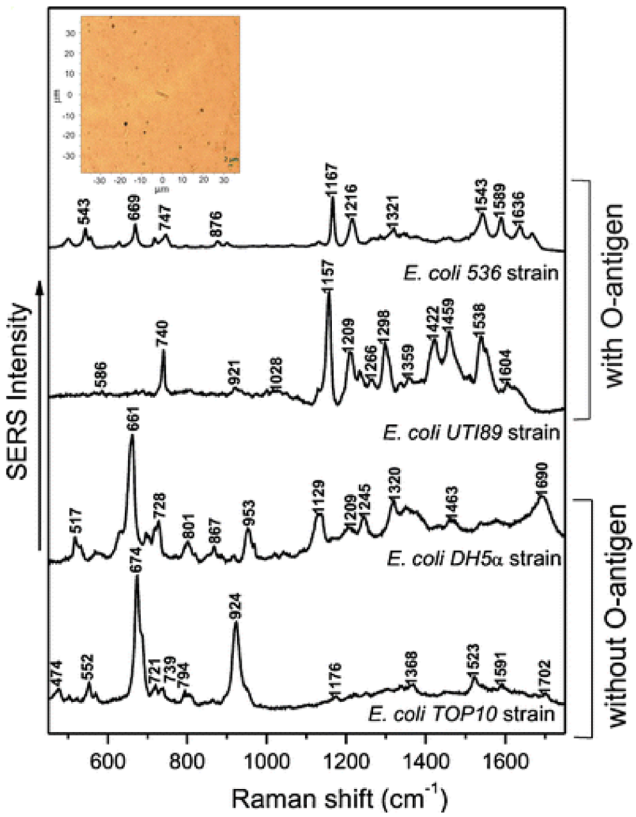

Fig. 5 Single-bacterium SERS spectra of rough strains (without O-antigen: DH5α and TOP10) and of smooth strains (with O-antigen: UTI89, 536), respectively. Inset, microscopic image of the tested *E. coli* DH5α rough strain. The image is reprinted from Mircescu *et al.*,[81] Copyright (2014), with permission from Springer.

blood samples. Liu *et al.* designed vancomycin-coated AgNPs arrays for the direct SERS detection of vancomycin sensitive and resistant *Enterococcus* species in blood samples.[82] Vancomycin captured the bacterial cells from blood to a SERS "hot junctions" surface, thereby enabling sensitive detection. The capture was due to the formation of hydrogen bonds between the bacteria cell wall's peptidoglycan and the vancomycin's carbonyl/amine groups. The blood cells most likely did not adhere to the vancomycin-coated surface and were removed by washing steps, which eliminated their SERS spectral contributions. The SERS spectra of resistant strains were not altered by the adhesion to the vancomycin-coated surface. While distinct spectral changes were noticed for the susceptible strains. These results represented a step towards the creation of SERS-based multifunctional biochips for the rapid and less complicated culture- and label-free detection of antibiotic resistant bacteria in real life samples.

Another research direction to evaluate the antibiotic resistance is to perform antibiotic susceptibility testing (AST) to understand the effectiveness of antibiotic treatment against bacterial infection. This will determine the minimum inhibitory concentration (MIC) of the antibiotic that prevents the bacterial growth. The MIC determination through conventional AST methods requires overnight bacterial culture, which is not ideal

for the real-time pathogen susceptibility measurements. SERS-based AST can eliminate the need for overnight culture and reduce the testing time, as it can rapidly assess the response and the susceptibility of bacteria to the antibiotic treatments.[83–85] In turn, this will be helpful in understanding the mechanism of action and effectiveness of antibiotics in a short time and allow a rapid decision to be taken by the physicians.[86]

A large number of antibiotics are designed to target the bacterial cell wall. Therefore, upon the antibiotic treatment, the biochemical composition of the bacterial cell wall is expected to disrupt, giving rise to secretion of intracellular components, thereby changing their spectral pattern which can be interpreted by SERS.[65] For example, Liu *et al.* reported a high speed SERS platform made of AgNPs embedded in anodic aluminum oxide with nanochannels for the detection of antibiotic sensitivity of *E. coli* and *S. aureus* at single bacterium level.[87] A characteristic changes in SERS spectral profile of the bacteria was observed within one hour after antibiotic exposure, which can be used for the early differentiation of the antibiotic susceptible strains from the resistant ones. Interestingly, the method managed also to report the fine changes in the bacterial cell wall during the bacterium's different growth stages. In another study, a SERS substrate based on 2D hexagonally packed AgNPs embedded in nanochannels of anodic aluminum oxide was used to determine the AST and MIC of different bacteria.[88] After exposing *MSSA* and clinical isolates of *MRSA* to oxacillin, the SERS signal intensity of *MSSA* dropped within two hours while the SERS signal of *MRSA* remained unchanged. This was attributed to cell wall degradation by oxacillin. Similar results were obtained for susceptible and resistant *E. coli* strains upon treatment with imipenem. Additionally, the SERS-active substrate was explored to establish MICs for clinical isolates of other species. *MRSA* clinical isolates were treated with vancomycin, while *E. coli*, *A. baumannii*, and *K. pneumonia* isolates were treated with imipenem. Imipenem and vancomycin inhibited the cell wall synthesis and inactivated the bacteria. The obtained results were in good agreement with that obtained using the traditional culture-based methods. However, the SERS method offered AST on viable bacteria and quantitative determination of MIC in a very short time, compared to standard culture-based methods that can take up to 24 hours to complete.

In another application, SERS was used to understand the mode of action of different antibiotics toward bacteria. The antibiotic response of *Lactococcus lactis* against ampicillin and ciprofloxacin was tested using 50 nm AuNPs colloidal solution.[89] Both antibiotics induced different spectral changes on the bacterial cell wall which revealed detailed biochemical information on bacterial responses and susceptibility. After 60 min of antibiotics exposure, ciprofloxacin induced only minor changes, while ampicillin induced significant SERS spectral changes. This was attributed to the mechanism of action of ciprofloxacin that disrupts DNA synthesis, and hence, the cell wall integrity was maintained for longer and its SERS spectrum remained stable. While ampicillin interrupts the cell wall synthesis, which was directly detected by the SERS-active AuNPs. This rapid and simple study demonstrated that SERS not only senses the changes in the bacterial cell wall, but also reveals details of the bacterial biochemical profiles, which help to understand how bacteria respond to antibiotics during early antibiotic treatment.

To simplify sample preparation steps in SERS based-AST method, Liao *et al.* in a very recent study proposed a prototype automated microfluidic control system to integrate reagent replacement, bacteria trapping and buffer exchange into a single device (Fig. 6).[90] This *in situ* SERS-AST was performed by

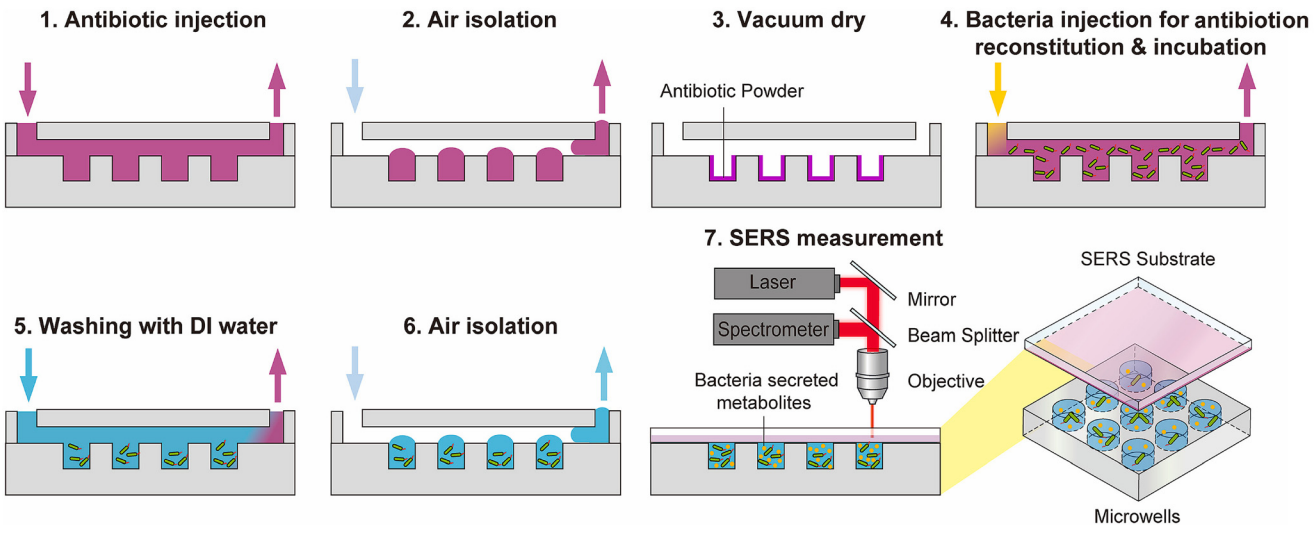

Fig. 6 The SERS–AST protocol operated by the automated microfluidic control system. The protocol can be divided into four parts comprising seven steps: (1) "antibiotic preloading", including antibiotic injection, isolation, and drying (steps 1–3). (2) "bacteria injection for antibiotic reconstitution and incubation" (step 4). (3) "DI water washing and air isolation" (steps 5 and 6). (4) SERS substrate attachment for multi parallel *in situ* "SERS measurement" (step 7). The image is reprinted from Liao *et al.*,[90] Copyright (2021), with permission from Elsevier.

loading isolates of susceptible and resistant *E. coli* with ampicillin for 3.5 hours. A clear discrimination between the two strains under antibiotic treatment was obtained. The developed system demonstrated a standardized and simplified SERS-AST protocol and implicated a parallel bacterial detection. The limitation of this setup is the low throughput for the spectra measurement. This can be improved by integrating a control program of motorized stage with spectral measurement. Another direction for improvement is to increase the bacterial distribution uniformity by optimizing the microwells dimensions. Additionally, to install a microfluidic concentration gradient generator to load antibiotics of various concentrations for multiplex AST.

To conclude, several studies confirmed that SERS has the power to detect and discriminate between different pathogenic strains for antibiotic resistance diagnosis in a comparable manner with other traditional techniques that are already used at POC. The sensitivity and speed benefits of SERS could enable the clinician to prescribe tailored antibiotics to improve healthcare and save financial resources. Additionally, the use of intelligent analysis for the spectral data would improve the discrimination power of the technique.[91] In the next section, the recent innovations in SERS applications that have been described for the detection of the "*Big 5*" antibiotic resistant challenges are discussed. A summary of these SERS approaches that included within this review is provided for the reader in Table 1. Interestingly, the vast majority of these approaches were developed in the last 5 years which indicates how SERS is showing a notable advance towards the monitoring of antibiotic resistance.

4. SERS applications for the "*Big 5*" antibiotic resistance challenges

4.1. *Methicillin resistant Staphylococcus aureus* (*MRSA*)

MRSA is one of the leading clinical threats to public health. It is transmitted easily in hospitals and can cause bacteraemia, endocarditis, skin infection, bone and joint infections. Even with the ongoing development of new antibiotics and advances in infection control and prevention, *MRSA* remains a prominent pathogen with persistently high mortality. Therefore, effective management is essential to mitigate its effect.[92]

Several SERS platforms have been designed for the rapid, sensitive and selective detection of *MRSA*. For example, Zhang *et al.* demonstrated the use of SERS for the evaluation of *MRSA* sensitivity to antibiotics and polymicrobial infection.[93] In this study, a plasmonic nanostructure live bacterial SERS platform was fabricated for the sensitive *in situ* monitoring of nitric oxide (NO) release from an individual *MRSA* upon antibiotic stress. AgNPs were modified on the bacterial surface as a plasmonic antenna and anchored with SERS reporter 2,2′-disulfanediylbis(*N*-(2-aminophenyl)acetamide). The platform was highly selective, sensitive and provided a fast responsive towards NO recognition. By external stimulation for *MRSA* with ampicillin and vancomycin, the bacteria generated NO in a concentration dependent manner which cleaved the SERS reporter to form free benzotriazole and carboxyl groups, leading to a strong SERS signal variation for effective biosensing. In the absence of antibiotics, there was no noticeable difference in the signal of the SERS reporter, indicating that there was no detectable amount of NO released from *MRSA.* Moreover, the method demonstrated the *in situ* SERS imaging of NO release at a single *MRSA* level in a polymicrobial infection model when co-cultured with *P. aeruginosa*. Therefore, this method offered more understanding of NO generation in different bacterial physiological process. Additionally, it presented a new SERS platform for the sensing (less than 100 nM) of various bacterial secretions under different conditions.

SERS was also combined with other techniques for the sensitive detection and rapid differentiation of *MRSA* with other strains. Lu *et al.* designed a microfluidic chip coupled with SERS as an optofluidic-based SERS system for the rapid detection of *MRSA* and for the differentiation between *MRSA* and *MSSA* in clinical specimens.[79] The clinical isolates were first analysed with PCR and multilocus sequence typing (MLST) to identify the *mecA* gene that is present in all *MRSA* isolates. A microfluidic device of T-junction geometry with a syringe pump system was used to inject AgNPs, NaCl (aggregating agent) and bacterial suspensions under a controlled flow for mixing the reagents inside the device channels. The recorded variations in the SERS spectral features between both strains were used for the differentiation between *MRSA* and *MSSA*. In addition, a partial least squares regression (PLSR) chemometric model was used to accurately determine the actual concentration of *MRSA* when present in a mixture with *MSSA*. The described optofluidic platform offered a much more rapid analysis time when compared with PCR and MLST.

Another combined platform was reported for the duplex assay of *MRSA* specific genes (*mecA and femA*) using SERS-PCR approach.[94] In this method, the genomic DNA extracted from *MRSA* clinical specimens was amplified by PCR targeting the *femA* and *mecA* genes. By using primers containing 5′ overhang sequence, a successful hybridisation with the capture sequence on two different SERS nanotags can be performed, leading to specific labelling of *femA* and *mecA* amplicons with their corresponding SERS nanotags. Then, streptavidin magnetic beads were reacted with the biotinylated PCR amplicons and finally forming a sandwich complex with the corresponding SERS nanotag. The formed complexes were then magnetically separated and detected by SERS to record the fingerprint spectra corresponding to the specific genes. The limit of detection was 1 and 4 DNA copies for *femA* and *mecA* genes, respectively. Compared to traditional gel electrophoresis methods, the proposed SERS-PCR assay offered the advantages of sensitivity, speed and multiplexed capability.

Another duplex system for the detection of *femA* and *mecA* genes was described by Restaino and White.[95] They reported the first design of a real-time PCR-SERS thermoplastic microsystem that allows simultaneous nucleic acid amplification and product separation into a SERS-active silver colloid for the real-time detection. In this system, a laser cut thermoplastic

Table 1 A summary of SERS approaches discussed within this review for the "*Big 5*" antibiotic resistant challenges

Target	Assay summary	Ref.
MRSA	Monitoring of nitric oxide release from *MRSA* upon antibiotic stress (30 min) (LOD less than 100 nM)	93
MRSA	Optofluidic-based SERS system to detect *MRSA* and differentiate between *MRSA* and *MSSA* species (25–30 min)	79
MRSA	SERS-PCR duplex assay of *MRSA* specific genes (*femA* and *mecA*) (1.5 h) (LOD 1 and 4 input DNA copies, respectively)	94
MRSA	Real-time PCR-SERS thermoplastic microsystem for the duplex detection of *femA* and *mecA* genes	95
MRSA	Label-free NIR-SERS assay of *MRSA* with other pathogens (>5 min) (LOD 10^3 CFU mL^{-1})	96
MRSA	Label-free SERS detection of *MRSA* with other bacteria using vancomycin-modified Ag-coated magnetic nanoparticles with secondary Au@AgNPs (<30 min) (LOD 5×10^2 cells per mL)	97
MRSA	Multiplex SERS detection of *MRSA* with other species using lectin functionalised magnetic nanoparticles (1 h) (LOD 10 CFU mL^{-1})	20
MRSA	Identification of *MRSA* using SERS and machine learning techniques	99
MRSA	Identification of *MRSA* using SERS and deep learning techniques	100
MRSA	Synergistic approach based on Au–Ag nanoshells-mediated photothermal therapy with SERS detection of residual bacteria (10 min) (LOD 300 CFU mL^{-1})	101
MRSA	Synergistic SERS effect of antibacterial curcumin liposome@AuNPs nanocomposite structure and AgNPs for the dynamic monitoring of bacterial bacteriostatic process	102
CRE & *ESBLs* (*K. pneumonia*)	SERS identification of *K. pneumoniae* with other pathogens after lysis filtration using a handheld spectrometer (4–5 h) (LOD 10^9 CFU mL^{-1})	107
CRE & *ESBLs* (*K. pneumonia*)	SERS Identification of *K. pneumoniae* with other pathogens using AgNPs-decorated filter membrane and pattern recognition techniques	108
CRE & *ESBLs* (*K. pneumonia*)	Label-free SERS method for discrimination between carbapenem-resistant and sensitive strains using computational analysis for SERS spectral data	109
CRE & *ESBLs* (*K. pneumonia*)	Label-free sensing and effective photothermal bacterial killing using 3D plasmonic SERS substrate design (5 min) (LOD 5 CFU mL^{-1})	110
CRE & *ESBLs* (*K. pneumonia*)	Sandwich based-SERS assay using boronic acid-functionalized polydopamine-coated Au@AgNPs and modified magnetic IgG@Fe_3O_4 nanoparticles (30 min) (LOD 10 CFU mL^{-1})	111
CRE & *ESBLs* (*E. coli*)	Sandwich based-SERS assay using AuNPs-coated starch magnetic beads functionalised with a linker protein (LOD 1 CFU mL^{-1})	118
CRE & *ESBLs* (*E. coli*)	Aptamer-based biosensor as a single selective probe for SERS detection of *E. coli O157:H7* (15 min) (LOD 10 CFU mL^{-1} in pure culture)	120
CRE & *ESBLs* (*E. coli*)	Au nanostars conjugated with ceftriaxone as a beacon for SERS detection of *New Delhi metallo-betalactamase*-producing *E. coli* (25 min)	121
CRE & *ESBLs* (*E. coli*)	Phenotypic detection of β-lactamase activity using paper SERS sensor and portable instrumentation (LOD 10^5 CFU)	122
TB	SERS detection of *TB* biomarker (ManLAM) in pre-treated human serum samples (LOD 2 ng mL^{-1})	126
TB	SERS detection of *TB* biomarker simulant (PILAM) in pre-treated human serum samples (LOD 10 pg mL^{-1})	127
TB	SERS detection of PILAM using benchtop and handheld instrumentation (LOD 0.032 and 0.18 ng mL^{-1}, respectively)	128
TB	Electrochemical-SERS aptasensor platform for label-free SERS detection of *TB* DNA biomarker in urine (LOD 280 μg mL^{-1})	130
TB	SERS-chemometric detection of *TB* biomarker (mycolic acid) using a closed lab-on-a-chip system (1 h)	80
TB	SERS Identification of different mycolic acid forms using Ag coated silicon nanopillar substrates and chemometric data analysis	131
TB	SERS identification of secreted metabolites of different mycobacteria species using sensible functional linear discriminant analysis	132
TB	SERS-multivariate statistical methods for healthy and *TB* infected serum samples using different SERS substrate design	133
TB	Diagnosis of active and latent tuberculosis infection using SERS and Raman spectroscopy combined with statistical rationale	134
VRE (*E. faecalis*)	Diagnosis of bacterial pathogens in urine using cylindrical SERS chip and recognition software. PCA model to identify susceptible and resistant strains and to diagnose mixed-flora infections	139
VRE (*E. faecalis*)	SERS identification of *E. faecalis* and other bacteria in urine using 50 nm gold-coated membrane filters and PC-LDA chemometric model (15 min) (LOD 10^5 CFU mL^{-1})	140
VRE (*E. faecalis*)	SERS identification of Gram-positive and Gram-negative bacteria *via* re-crystallization of AgNPs in solution and cluster analysis (15 min)	141
VRE (*E. faecalis*)	Multifunctional nanocomplex for SERS detection and antimicrobial photodynamic therapy of *VRE* strains	142
VRE (*E. faecium*)	SERS-3D PCA detection of *E. faecium* and other Gram-negative pathogens using positively charged columnar array of Au@Ag nanorods and Au nanoplate-nanosphere assemblies (LOD 100 CFU mL^{-1})	144
VRE (*E. faecium*)	Organometal-based SERS method used electrochemical deposition onto plasmonic metal nanopillars Au substrate for the detection of bacterial DNA of *E. faecium* and *S. aureus* (LOD ~0.035 nM) (<10 min)	145
NG	SERS detection of enriched bacterial cellular suspensions using SiO_2 substrates covered with AuNPs and AgNPs (<1 hour) (LOD 10^5 CFU mL^{-1})	11
NG	SERS-chemometric analysis of *NG* and other pathogens in men's urethra swabs using silicon substrates sputtered with Ag layer (<15 min) (LOD 10^2 CFU mL^{-1})	146

fluidic chip has been devised to utilize a dialysis membrane capable of isolating a PCR reaction from the AgNPs clusters. As the reaction progresses, a Raman reporter-labelled DNA probe is degraded, liberating the reporter from probe DNA, allowing passage across the size-restricting dialysis membrane into the SERS-active colloid, where the accumulating reporter can be measured in real-time. Dialysis eliminated the post-processing steps through isolation of the SERS colloid from the PCR reaction. Therefore, the design enabled simple and real-time identification of *femA* and *mecA* genes simultaneously in a single PCR-SERS reaction and from a single well.

SERS was also used for the multiplex detection of *MRSA* with other bacterial pathogens. For example, Chen *et al.* reported a label-free near *infra*-red-SERS (NIR-SERS) assay for the discrimination and detection of *MRSA* with *E. coli*, *P. aeruginosa* and *Listeria* spp. in drinking water *via in situ* synthesis of AgNPs within bacterial cell suspensions.[96] The pre-treatment of bacterial cells with cell membrane disruption reagent Triton X-100 resulted in new features on their SERS spectra attributed to the inner components of the bacterial cell wall, allowing for a successful discrimination. Furthermore, the method was able to distinguish between two *MRSA* strains from clinical isolates. Although the method required very low sample volume (5 μL) and less than 5 min to perform the assay, the used bacterial concentration may potentially obscure the relative peak intensity and the baseline intensity. Additionally, different strains shared some identical features and only show minor spectral difference. Modifying the substrate surface and using microfluidics with the proposed *in situ* approach can avoid spectral interference from mixed bacterial samples and achieve uniform concentration of bacteria.

Another recent study was reported by Wang *et al.* for the label-free SERS detection and differentiation of *MRSA*, *E. coli* and *S. aureus* using vancomycin-modified Ag-coated magnetic nanoparticles (Fe_3O_4@Ag-Van MNPs) with secondary Au@AgNPs.[97] Fe_3O_4@Ag-Van MNPs were used for the bio-recognition of the bacteria in a complex sample. After capturing the bacteria, the Au@AgNPs were spread over the Fe_3O_4@Ag-Van–bacteria complexes for further SERS signal enhancement. The measurements were recorded *in situ* and the resultant SERS spectra of the bacteria show some similar features. Therefore, PCA was performed on the multiplex spectrum to support the successful identification and discrimination between the pathogens. This dual enhanced strategy demonstrated high bacterial capture efficiency (>65%) within a wide pH range (pH 3–11), short assay time (<30 min) and low detection limit (5×10^2 cells per mL). Moreover, the spiked tests show that this method is still applicable in milk and blood samples. A similar approach was also reported by Kearns *et al.* for the multiplex SERS detection of three bacterial pathogens (*MRSA*, *E. coli* and *S. typhimurium*) using lectin functionalised magnetic nanoparticles for the extraction of bacteria from the sample matrix.[20]

The rapid SERS diagnosis of antibiotic resistance is advantageous. However, SERS spectra interpretation is sometimes difficult due to the high molecular similarities between antibiotic-resistant and susceptible species. The integration of advanced data analysis techniques with SERS data can overcome this difficulty and enable rapid, accurate and reproducible discrimination.[98] In a recent study, Ciloglu *et al.* applied machine learning techniques with SERS for the rapid and reproducible identification of *MRSA*, *MSSA* and Gram-negative *Legionella pneumophila* (control).[99] PCA, hierarchical cluster analysis (HCA) and various supervised classification algorithms were used to discriminate between the pathogens. The SERS spectra of each bacterial sample exhibited great reproducibility and high signal-to-noise ratio. Although there wasn't much spectral difference between the *MRSA* and *MSSA*, the intensity ratios of some peaks could be used to show the difference between the strains. The k-nearest neighbours (kNN) classification algorithm showed superior classification performance with 97.8% accuracy among the other traditional classifiers. In a more recent study,[100] the same group proposed a deep neural network (DNN) that can discriminate between antibiotic resistant bacteria using SERS. Stacked autoencoder (SAE)-based DNN was used for the rapid identification of *MRSA* and *MSSA* using a label-free SERS technique (Fig. 7). Since SERS provided high signal-to-noise ratio, some subtle differences were found between *MRSA* and *MSSA* in relative band intensities. SAE-based DNN can learn features from raw data and classify them with an accuracy of 97.66%. Moreover, the model discriminated the bacteria with an area under curve (AUC) of 0.99. Compared to traditional classifiers, SAE-based DNN was found superior in accuracy and AUC values. These results indicated that deep learning algorithms can successfully discriminate the antibiotic resistant bacteria by using SERS data. Additionally, it demonstrated the great potential for a lot of label-free SERS applications in the biomedical field.

In another application, He *et al.* reported the use of SERS as a preliminary theranostic tool to diagnose and combat against *MRSA* and antibiotic resistant strains of *E. coli*.[101] They synthesised Raman tag (3,3′-diethylthiatricarbocyanine iodide)-conjugated gold-silver nanoshells (DTTC-AuAgNSs) as a substrate. The laser irradiation of the substrate released silver ions which exhibited an efficient photo thermal effect that can eradicate both *MRSA* and *E. coli*. Additionally, the synthesised substrate was used for the SERS imaging to provide a non-invasive and highly sensitive detection of *MRSA* down to 300 CFU mL^{-1}, as well as a prolonged tracking of residual bacteria at least for 8 days. Additionally, in a chronic *MRSA* infected wound mouse model, the AuAgNSs gel-mediated photo thermal therapy/silver-release lead to a synergistic wound healing with negligible toxicity or collateral damage to vital organs.

Similarly, in a very recent study conducted by Xiang *et al.*, antibacterial nanocomposite structure combined with AgNPs as a SERS substrate was applied as a synergistic approach for the dynamic monitoring of bacteriostatic process of *MRSA* species.[102] A curcumin liposome@AuNPs nanocomposite was designed and used as bacteriostatic agent, as well as a SERS probe. By means of electrostatic attraction between the nano-

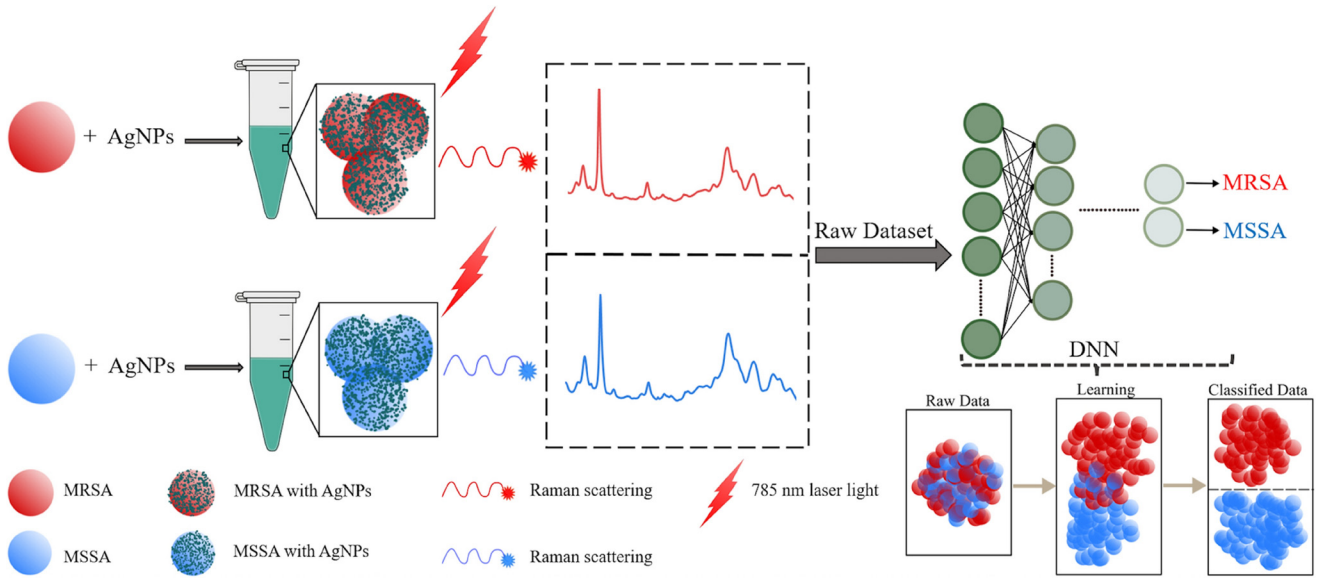

Fig. 7 General workflow of deep learning-based spectral data analysis for the discrimination of *MRSA* and *MSSA*. The image is reprinted from Ciloglu *et al.*,[100] Copyright (2021), with permission from Springer Nature.

composite and *MRSA* onto the surface of the AgNPs substrate, a specific detection of *MRSA* at the molecular level was simply realized by SERS. Additionally, the changes in the bacterial structure after bacteriostatic effect were monitored. Furthermore, the important intermediates produced during the bacteriostatic process were also measured.

These results suggested that the developed SERS nanoshells/nanocomposite could demonstrate a convenient, effective and safe inhibition to bacterial infection and a promising potential for clinical translation. Nevertheless, comprehensive toxicity studies on human cells and histological evaluation of major organs are required on a larger scale before implementing such approaches for real clinical samples.

4.2. *Carbapenem resistant Enterobacteriaceae* (*CRE*) and *Extended-spectrum beta lactamases* (*ESBLs*)

Enterobacteriaceae are considered as a large family of Gram-negative bacteria including a number of pathogens that can result in life-threatening complications.[103] To resist the effects of the antibiotics, some *Enterobacteriaceae* species can release extended-spectrum beta lactamase (ESBL) enzymes that inactivate the effect of some beta lactam antibiotics (*i.e.*, penicillins and cephalosporins) towards the infection.[103] Carbapenems are one of the few remaining antibiotics that still can treat ESBL-producing bacteria and referred to as the last line of antibiotic treatment against resistant organisms. However, *Enterobacteriaceae* can stop the action of carbapenems forming *carbapenem resistant Enterobacteriaceae* (*CRE*). Therefore, *CRE* are considered a real critical threat to the public health.[104] Amongst ESBL-producing *Enterobacteriaceae* or *CRE*, the major concerns are attributed to *K. pneumonia* and *E. coli* as they have become serious clinical problems worldwide.[105,106]

Due to its speed, sensitivity and simplicity, SERS was presented in different studies as a promising alternative diagnostic tool for the detection of these bacteria instead of using the lengthy culture methods and sophisticated PCR technique. In this section, we highlight some recent advances in the SERS detection of *K. pneumonia* and *E. coli* as demonstrators for *CRE* and ESBL producing *Enterobacteriaceae*.

Kotanen *et al.* presented a method to characterize and evaluate a handheld SERS-based diagnostic system for the detection and identification of *K. pneumonia* with other bacteria (*E. coli*, *P. aeruginosa*, *Acenitobacter baumannii* (*A. baumannii*) and *S. aureus*) in pooled human sera.[107] The bacterial species were inoculated into pooled human serum samples, then lysis filtration was used to separate the bacteria. The isolated bacteria were incubated onto AgNR substrates at 60 °C for 3 hours and scanned with a handheld Raman spectrometer. The resultant spectra were compared to pure culture bacteria spectra as a reference library using statistical analysis. The bacterial species were identified and distinguished by their SERS fingerprints at the species level. Although the lysis filtration was able to purify the hydrophilic bacteria without significant changes on their Raman spectra, bacteria sensitive to lysis filtration still require a reference library for their SERS identification or even milder separation conditions. Additionally, shifts in the relative peak intensities were noticed due to the sample loss during lysis filtration. Furthermore, the effect of serum filtration on the SERS spectra of poly-microbial populations needs to be addressed.

Similarly, Lin *et al.* reported another SERS method for the rapid detection of *K. pneumonia* with *Salmonella* and *A. baumannii*.[108] The combination of a AgNPs-decorated filter membrane, as a SERS substrate, with pattern recognition techniques enabled a good bacterial classification with respect to

rapid and low-cost clinical diagnostics. The prediction ability of the method to classify the bacteria SERS spectra reached 100% using a leave-one-out cross-validation (LOOCV) procedure. Nevertheless, the method only presented a preliminary study and further improvements are required. For example, there is a need to set a more comprehensive library that include more bacteria, bacteriophages and other clinical isolates to minimize other biomolecules interference on the selectivity and sensitivity of the assay when performed in a more complicated mixture.

In another recent pilot study, Liu *et al.* reported a label-free SERS method for the discrimination between clinically isolated carbapenem-resistant and carbapenem-sensitive *K. pneumoniae* strains using computational analysis for their SERS spectra.[109] A total of eight supervised machine learning methods were performed on SERS spectral data and compared in terms of their capacities in predicting the resistant and sensitive strains. Among these algorithms, convolutional neural network (CNN) enabled high computational efficiency, strong fault tolerance and achieved 99.78% prediction accuracy with a good robustness on low signal-to-noise ratio data when compared with other supervised machine learning algorithms. Although the high prediction accuracy, there are still many aspects that need to be improved for the potential application of this method in clinical settings. For example, the used models are not robust and sufficient for real-world applications due to the limited number of *K. pneumoniae* strains used in the study. More SERS spectra from clinically isolated strains should be used for training the machine learning models, which would improve the robustness of the models. In addition, antibiotic resistance profiles during *K. pneumoniae* isolation should be strictly controlled, and those strains only with differences in carbapenem sensitivity and resistance should be used for SERS spectral analysis. Therefore, machine learning models could reliably predict sensitive and resistant strains solely based on carbapenem resistance rather than other antibiotic resistances.

In another application, a 3D plasmonic SERS substrate design was reported for the label-free sensing and effective photothermal killing of *K. pneumonia* and *A. baumannii*.[110] The 3D substrate was fabricated by the attachment of AuNPs to a hybrid graphene oxide surface. The experimental results indicated the 3D substrate can be used for the fingerprint sensitive detection of several multi-drug resistant superbugs with detection limits of 5 CFU mL^{-1}. Additionally, the 3D substrate enabled a rapid and effective killing of 100% of the bacteria within 5 min at 785 nm NIR light exposure. Therefore, this 3D substrate demonstrated a promising theranostic approach for multi-drug resistant superbugs. However, the utilisation of such platform in the photothermal killing of superbugs for real clinical applications can produce different results with different bacteria. Therefore, more optimisation and validation studies are required in the presence of different types of pathogens in complex clinical matrices before the assay can be adopted for POC. Furthermore, some practical problems such as, metallic nanostructures cytoxicity, NPs aggregation in human blood, formation of protein corona and inefficient renal clearance still need to be solved first.

In another recent application, a sandwich assay was reported for the detection and classification of *K. pneumonia* with *S. aureus*, *E. coli*, *Shigella dysenteriae* and *P. aeruginosa*.[111] In this assay, modified magnetic IgG@Fe_3O_4 NPs were used for the bacterial separation as IgG has high affinity towards protein A, protein G, protein L and glycans on the surface of bacterial cells. Boronic acid-functionalized polydopamine-coated Au@Ag NPs containing 4-aminothiophenol (pATP), as a reporter, were used a SERS tag. Boronic acid is an effective bacterial capture molecule that could specifically bind to the bacterial diol group of the saccharide. Therefore, in the presence of the bacteria, the sandwich complex was formed and the Raman signal of pATP was amplified. The resultant SERS spectra from different bacterial species were analysed using PCA and HCA and indicated that the regions attributed to surface protein and glycan (1300–1450 cm^{-1}) were the best regions for bacterial classification. The lowest limit of detection was 10 CFU mL^{-1}. Although this assay can be completed in 30 min, it can be used only for the detection of pure bacteria with high binding affinity towards IgG. Bacterial complexes or bacteria with low IgG binding affinity cannot be detected by this method.

The SERS detection of the other *CRE* model, *E. coli*, has been extensively reported using different approaches.[112–117] For example, a typical sandwich based-SERS assay was recently reported for the SERS detection of *E. coli O157:H7* using AuNPs-coated starch magnetic beads (AuNPs@SMBs).[118] The AuNPs@SMBs were functionalised with a linker protein, gold-binding peptide-tagged Staphylococcal protein G (GBP-SPG), for the immobilisation of specific capture antibody. A compatible SERS tag was prepared by functionalising AuNPs with a detection antibody *via* the linker protein GBP-SPG for the highly specific capture of *E. coli O157:H7*. The linker protein served also as a Raman reporter molecule due to its strong characteristic SERS signal. The reported detection limit was 1 CFU mL^{-1}. However, the method was applied in aqueous media and did not test the detection of the target pathogen in a multiplexed fashion with other relevant bacteria in real/simulated biological specimens.

In general, the sandwich based-SERS assay offers much higher sensitivity than direct SERS detection. In addition, the use of two recognition molecules for the bacteria is more efficient for the capture and detection in complex samples. However, in some cases the use of a secondary recognition molecule is not always possible, either due to unavailability or due to cost constraints. Another effective strategy for the selective detection of bacteria is to monitor the change in the SERS signal of a single capture probe after incubation with the target pathogen.[119] In a recent study, Díaz-Amaya *et al.* used an aptamer-based biosensor as a single selective probe for the rapid detection of *E. coli O157:H7*.[120] The biosensor was fabricated by the conjugation of 4-aminothiophenol-AuNPs with a selective DNA sequence for the specific capture and sensitive SERS detection of *E. coli O157:H7* in both pure culture

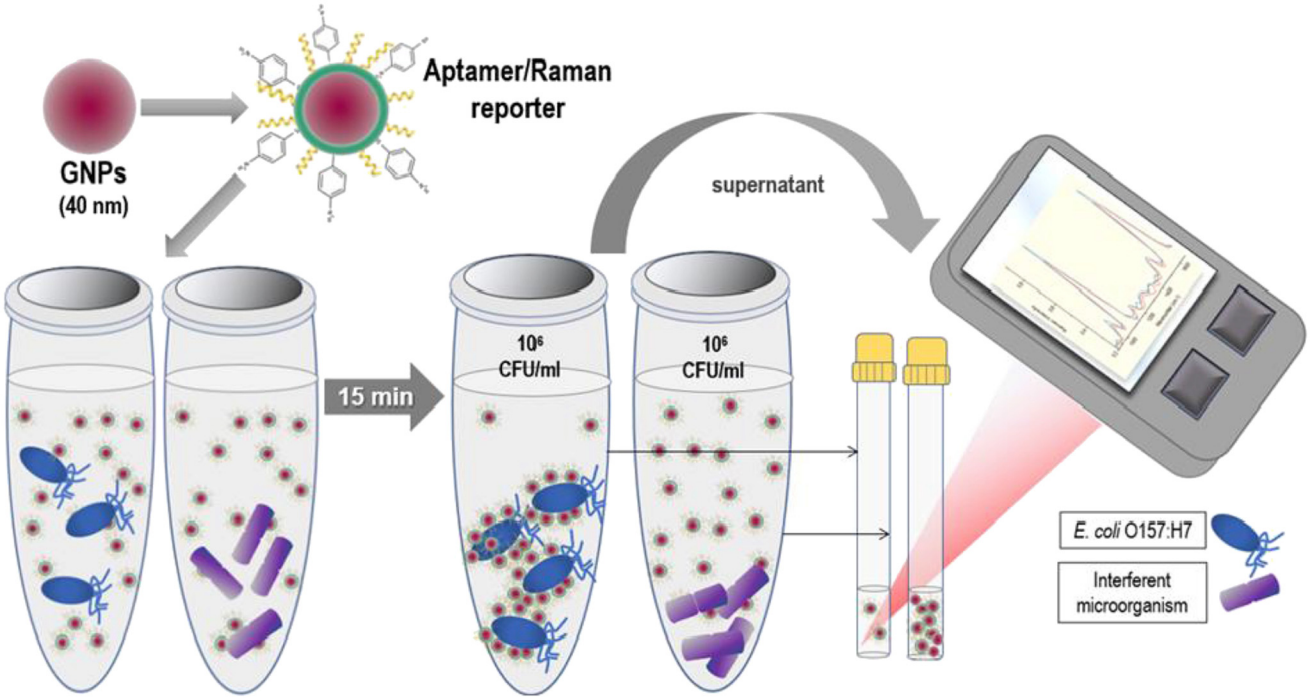

Fig. 8 Schematic illustration of the detection mechanism proposed for aptamer-based whole cell detection of *E. coli O157:H7*. The image is reprinted from Díaz-Amaya *et al.*,[120] Copyright (2019), with permission from Elsevier.

(~10 CFU mL^{-1}) and ground beef samples (~10^2 CFU mL^{-1}). By incubating the sample with the capture probe for 15 min, the probe-bacteria conjugate started to precipitate with time, resulting in a clear cell sedimentation and a superficial phase that contains unbounded capture probe (Fig. 8). By increasing *E. coli O157:H7* concentration, the number of Raman probes suspended in the supernatant layer was decreased, resulting in the reduction of 4-aminothiophenol SERS signal. Despite the high performance of the proposed biosensor compared to other conventional immune-based approaches, further system evaluations (*i.e.*, robustness, NPs size and shape modifications) under an extended set of experimental conditions are required before this approach could be applied for the on-site and simultaneous detection of different pathogens/strains in multiplexed samples.

In a different recent study, Wong *et al.* described another single capture probe for the detection of bacterial β-lactamase enzyme secreted by *New Delhi metallo-betalactamase* (NDM)-producing *E. coli*.[121] In this study, Au nanostars were conjugated with β-lactam antibiotic ceftriaxone (CRO) and used as a beacon for rapid detection. By incubating the NDM-producing *E. coli* with the conjugate for 25 min, a detectable reduction in the SERS signal intensity of CRO Raman peaks at 722, 1358, and 1495 cm^{-1} was noticed due to CRO hydrolysis by NDM-producing *E. coli* in spite of the fact that the rapid molecular structure change of CRO could be beneficial for early diagnosis and treatment, the method was not able to set a quantifiable limit of detection due to results variations between experiments using a one calibrated loop. Furtherly, the method was not applied for detecting the target bacteria in clinically relevant matrices that contain other interfering molecules.

In another application, CRO hydrolysis approach was also used for the discrimination between different ESBLs producing *Enterobacteriaceae* that show different resistance towards various cephalosporin generations.[122] The approach utilised a colorimetric molecular reporter for β-lactamase activity, CENTA, which designed to contain a β-lactam structure with a SERS barcode. As illustrated in Fig. 9, the hydrolysis of β-lactam rings in both of CENTA and CRO by ESBLs released sulfur-containing molecules that were used as SERS barcodes. These molecules were then placed onto a AgNPs paper SERS substrate for the SERS detection using a portable Raman spectrometer. CENTA, as a first generation cephalosporin demonstrator, is hydrolysed by all β-lactamase producing bacteria. Therefore, after 2.5 hours incubation with TEM-1 producing *E. coli* (resistant to first generation cephalosporins only), 5-thio-2-nitrobenzoic acid (TNB) was released and used as SERS barcode for the detection of TEM-1 strain. The most prominent peak in the spectrum was at 1334 cm^{-1} and attributed to the expected NO_2 stretch mode which confirmed the barcode release by hydrolysis. On the other hand, CRO, a third generation cephalosporin, was incubated with SHV-4 producing *E. coli* (resistant to third-generation cephalosporins and lower) and similarly released a free sulfur-containing barcode (Fig. 9). The most prominent peak after CRO hydrolysis was observed at 1366 cm^{-1}. Additionally, the incubation of *E. coli* that does not produce β-lactamase did not hydrolyse either CENTA or CRO and did not generate a characteristic SERS

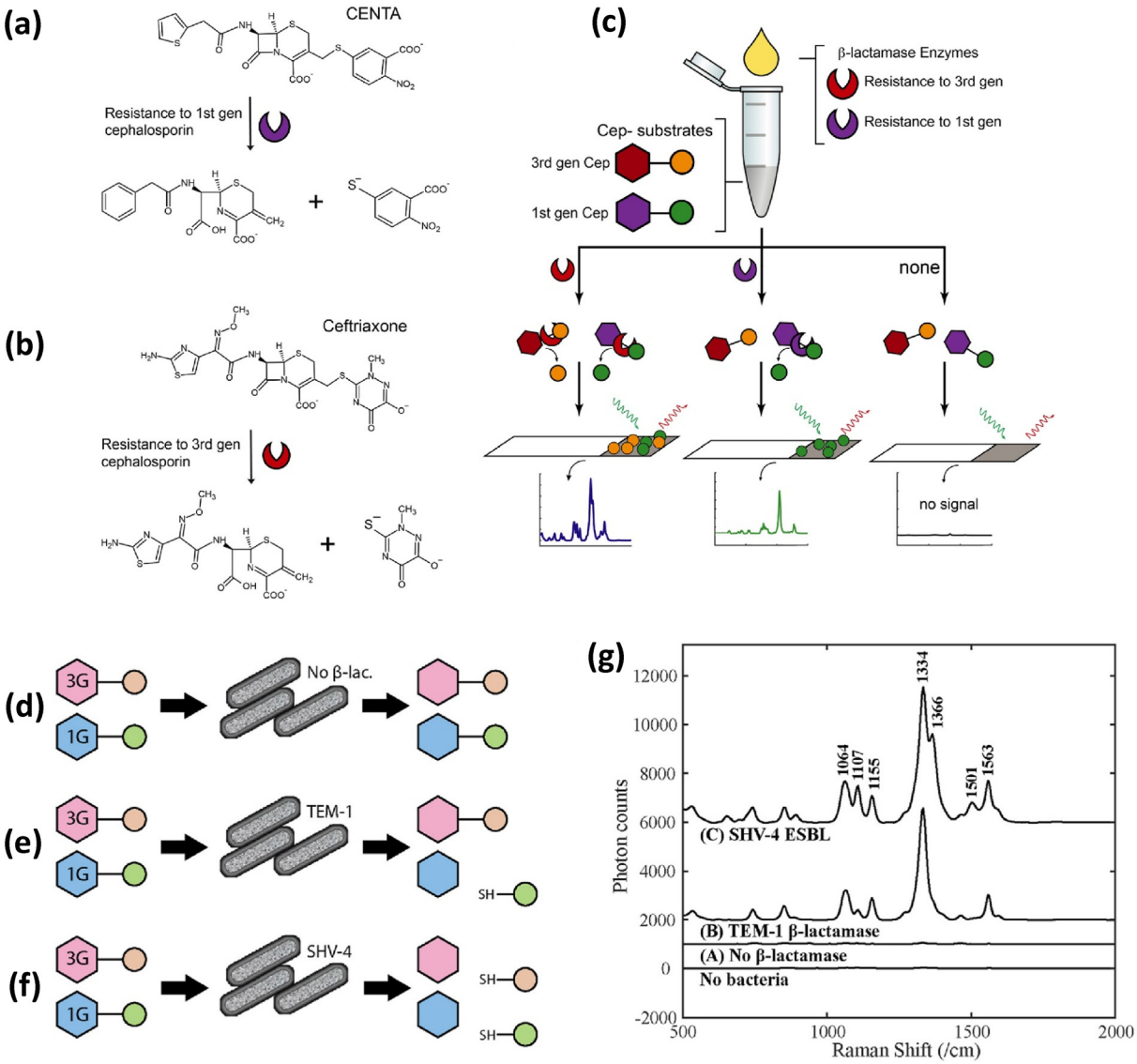

Fig. 9 (a) CENTA is hydrolysed by β-lactamases that promote resistance to first generation cephalosporins releasing a SERS barcode with a sulfur. (b) CRO is hydrolysed by *ESBLs* that promote resistance to third generation cephalosporins releasing a SERS barcode with a sulfur. (c) The reporter molecules are combined with a sample containing unknown β-lactamases; following incubation, the sample is added to a AgNPs paper SERS sensor. The resulting Raman spectrum indicates which barcodes were released through hydrolysis, thus revealing which generations of cephalosporins will not work against the pathogen. (d) *E. coli* that does not produce β-lactamase will not hydrolyse both reporters. (e) TEM-1 *E. coli* will hydrolyse the first generation reporter but not the third generation. (f) SHV-4 *E. coli* will hydrolyse both reporters. (g) SERS spectra show unique signals for the three different strains thus phenotypically differentiating the three strains by their β-lactamase activity. The images are reprinted from Hilton *et al.*,[122] Copyright (2020), with permission from Elsevier.

signal. The unique spectra for the two barcodes enabled a multiplexed detection for TEM-1 and SHV-4 producing *E. coli* with a limit of detection of 10^5 CFU. Therefore, this approach suggested that in a single sample and a single test, the most appropriate generation of cephalosporin for treatment can be identified in a short time due to the inherent multiplexing capability of SERS. While these two molecular barcodes demonstrated the potential to identify ESBLs resistance, the number of commercially available molecules that contain effective Raman barcodes attached to a cephalosporin *via* a sulfur is insufficient to represent all generations of cephalosporins. To expand this library, simple organic synthesis procedures can be applied to modify the barcodes to obtain additional SERS barcodes with distinguishable spectra.

4.3. *Mycobacterium tuberculosis* (*TB*)

Tuberculosis is a serious health condition that is caused by the inhalation of tiny droplets of *Mycobacterium tuberculosis* (*TB*) bacteria. It can still be cured if diagnosed accurately and treated efficiently with the right antibiotics. The current available diagnostic methods for *TB* include tuberculin skin test and interferon gamma release assays for the latent *TB* infec-

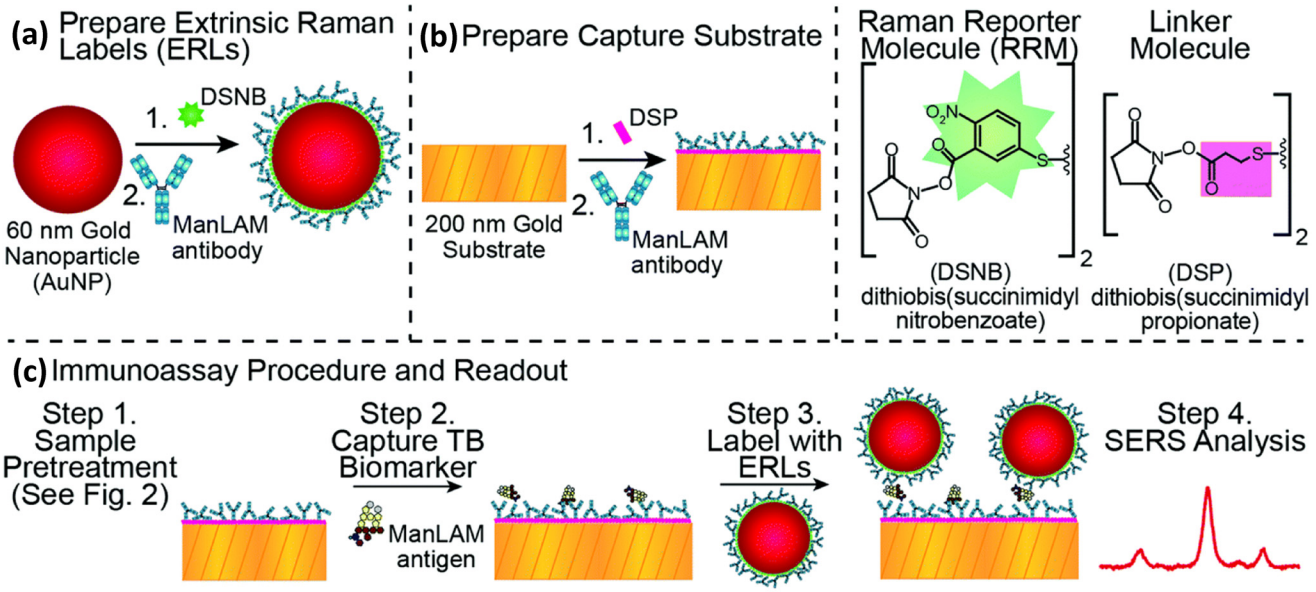

Fig. 10 The three main components of the SERS-based immunoassay approach for ManLAM detection: (a) ERL preparation, (b) capture substrate preparation, and (c) major assay steps. The assay is carried out by incubating a pre-treated serum sample (20 μL) at room temperature with the capture substrate. The samples are then rinsed, exposed to ERLs (20 μL), and analysed by SERS. The image is reprinted from Crawford *et al.*,[126] Copyright (2017), with permission from Royal Society of Chemistry.

tion, and sputum smear microscopy and culture/molecular methods for *TB* disease diagnosis. Although these methods provide reliable disease diagnosis and treatment monitoring, they are still associated with some challenges such as: low sensitivity and specificity, high cost, long turnover time, and skills requirement. Due to these challenges, several SERS diagnostic applications have been evolved for the early detection of *TB* biomarkers.[123,124]

For example, Porter's group developed multiple SERS based sandwich immunoassays demonstrating the importance of *TB* sample pre-treatment in enhancing the sensitivity of *TB* biomarkers detection in human serum samples.[125–128] For example, in the detection of the *TB* biomarker, mannose-capped lipoarabinomannan (ManLAM), in pre-treated human serum samples.[126] The sample pre-treatment step with perchloric acid disrupted the ManLAM complexes with proteins and other components in serum allowing the biomarker to be in its free form and thereby improve its detection sensitivity. As shown in Fig. 10, the ManLAM was then captured using a gold substrate functionalised with selective ManLAM antibody. Extrinsic Raman labels were bound to the biomarker using a linker forming the immunoassay and the reported LOD was 2 ng mL^{-1}. Although this proof-of-concept study demonstrated the potential of ManLAM to become an exciting addition to the TB diagnostics toolbox, this preliminary study still needs extensive series of validation studies to be carried out. Both the number of specimens and types of specimens must be markedly expanded.

The same concept was used in another study for the detection of phosphoinositol-capped LAM (PILAM) as a ManLAM simulant.[127] Rapid pre-treatment with perchloric acid was an effective way for releasing PILAM from complexation, enabling 1500× improvement in the LOD (10 pg mL^{-1}) when compared with the untreated serum sample. The same approach was associated later with a portable handheld Raman spectrometer in another PILAM assay to examine the next steps and potential processes required to move this immunoassay platform closer to POC.[128] The obtained results under different operational settings (*i.e.* signal integration time) for two Raman spectrometers were promising. The LOD when using a field-portable handheld spectrometer system (0.18 ng mL^{-1}) approached that of a benchtop instrument (0.032 ng mL^{-1}). However, there are a number of factors that need to be considered before this transition can occur, for example: the marked reduction in the time required to complete the assay and the design of reagent packaging, in terms of stability and cost. Additionally, more studies on the instrument performance and approaches to account for instrument-to-instrument variability are still required.

In another application, electrochemical-SERS (EC-SERS) approach has been successfully applied for the detection of *TB*.[129] For example, Karaballi *et al.* reported an EC-SERS DNA aptasensor platform for the label-free SERS detection of *TB* DNA biomarker in urine.[130] They used a cost-effective carbon screen printed electrode modified with AgNPs. The electrode surface was functionalised with target DNA recognition-aptamer to allow for selective hybridisation and backfilled with 12-mercaptododecanoic acid to avoid any nonspecific binding. The application of electrochemical voltage (−1 V) to the electrode had a considerable enhancing effect on the target SERS signal. The direct SERS detection of the target DNA was carried out through monitoring the SERS peaks of

adenine that appeared after target hybridisation, as adenine presents only in the target DNA. The reported detection limit was 280 μg mL^{-1} which is very high compared to that provided by PCR analysis of the DNA.

Another attractive biomarker for *TB* infection is mycolic acid (MA). MAs are long fatty acid chains that are characteristic to mycobacteria. They are stable, inert and of a high abundance in the bacterial cell wall.[131] Therefore, a number of SERS methods have been developed for the sensitive detection of MA as a marker for *TB* infection. Mühlig *et al.* developed a closed droplet based LOC device that has been integrated with SERS for the identification of 6 species of mycobacteria including *Mycobacterium tuberculosis* complex (MTC) and *nontuberculous mycobacteria* (NTM) through the monitoring of MA.[80] The mycobacteria cell wall was lysed using a bead-beating module, allowing for the release of cell wall bacterial suspension that contains MA. The bacterial lysate flowed onto AgNPs on the chip surface, in a closed system to enhance the safety, to acquire its SERS spectrum that is strongly dominated by contributions from MA. By using this design, more than 2100 individual SERS spectra from the bacterial suspensions were obtained in one hour. The SERS spectra from the different species were closely similar. Thus, two chemometric methods (PCA and linear discriminant analysis) were used to enable species discrimination.

Later, the three main forms of MA: αMA, methoxy-MA and keto-MA, were detected by SERS in delipidated MA, undelipidated MA samples and in gamma-irradiated whole bacteria without the need for extraction.[131] The spectra were collected using silver coated silicon nanopillar substrates and chemometric data analysis was employed for their differentiation. Again, this outlines the use of chemometric statistical analysis to aid SERS in the discrimination between similar Raman spectra of bacterial biomarkers so that minor spectral variations can be distinguished without additional extraction procedures. Thus, enabling rapid and reliable diagnosis of the bacterial infection.

In a recent study, Cheng *et al.* reported a new classification method called sensible functional linear discriminant analysis (SLDA) to identify different mycobacteria species based on the SERS spectra of their secreted metabolites.[132] Conventional PCA and linear discriminant analysis methods successfully separated the acquired spectrum of MTC from those of NTM species but failed to distinguish between the spectra of different NTM species. Therefore, SLDA was employed to effectively discriminate the MTC and different NTM species. All the SERS spectra of the tested NTM species were separated by the SLDA method with a nearly 100% accuracy.

Botta *et al.* reported a SERS-based detection method assisted by chemometric models to differentiate clearly between healthy and *TB* infected serum samples using slant, vertical, zigzag AgNRs and AgNPs.[133] However, the method was applied only for 2 clinical samples which is producing insufficient data to truly evaluate the method. Based on that, the same group reported a bigger scale study to distinguish *TB* infection in 4 groups: active *TB* cases, latent *TB* infection cases, early clearance and healthy controls.[134] The study was carried out using Raman spectroscopy (n = 118) and SERS (n for each *TB* infection category = 5). Despite the excellent diagnostic performance of SERS (100% accuracy) with promising cut-off values for differentiation among categories, the method used a limited number of pooled samples. Therefore, a further study with a higher number of samples is required for SERS analysis in the clinical application.

Overall, compared to other traditional techniques, the integration of SERS with different chemometric algorithms for complex spectral analysis offered the advantages of high sensitivity, convenient portability, short analysis time, low cost, easy automation, high-throughput analysis and most importantly uncomplicated successful discrimination between clinically relative species. However, before routine protocols and robust systems for this integration could be implemented, optimisation and evaluation of the models performance are essential. Additionally, samples validation by other reference methods are required on a large scale. Furthermore, trained staff are required to be familiarized with different statistical software, data interpretation and analysis, as well as be experienced in applying modified chemometric modules in real-time when needed.[135]

4.4. *Vancomycin resistant enterococci* (*VRE*)

Mostly, the *VRE* infection is clinically related to *Enterococcus faecalis* (*E. faecalis*) and *Enterococcus faecium* (*E. faecium*) bacterial infection. They are among the leading cause of several human infections, including septicaemia, urinary tract infections, wound infections, neonatal sepsis and meningitis.[136] Like other antibiotic resistant bacterial infections, the accurate diagnosis time is very crucial to start the therapy with the appropriate antibiotic treatment. For example, the survival rate of the patients with sepsis after 12 hours without appropriate therapy is below 20%.[137] Several techniques managed to shorten the diagnosis time, such as: MALDI-TOF MS, PCR, DNA microarrays and high throughput sequencing technologies. However, they are still showing some drawbacks as lack of sufficient reproducibility, laborious optimisations of protocols and lengthy sample preparations procedures.[137]

Different SERS studies were presented as rapid and reproducible methods for the identification and detection of *VRE* infection.[138] For example, a cylindrical SERS chip was developed for the rapid detection of urinary tract infection pathogens, *E. faecalis* and *E. coli*, in urine samples without a laborious sample process.[139] The cylindrical SERS chip was fabricated using AgNPs coated on the tip of a 2 mm polymethylmethacrylate rod and then illuminated by a portable Raman spectrometer. Previously isolated known bacteria from a conventional culture of patient samples were loaded on the SERS chip and used as a reference Raman spectrum and were confirmed by MALDI-TOF. A recognition software was then used to compare the SERS spectra collected from the measured samples with the reference spectra for quick pathogens identification with ≥95% fingerprint similarity. In addition, PCA was used to aid the diagnosis of mixed flora infections and to

differentiate between antibiotic susceptible and resistant bacterial strains. Due to the small number of available standard-reference Raman spectra from known bacteria for recognition software, a comprehensive Raman library and more PCA plots from combinations of the two different bacteria has to be established to accurately recognize patients' urine samples before this method can be widely used in the clinical diagnosis of urinary tract infection.

Similarly, Dryden *et al.* reported a recent study that used principal component–linear discriminant analysis (PC-LDA) with SERS to identify *E. faecalis*, *E. coli* and *K. pneumonia* infection in urine samples at clinically relevant concentrations (10^5 CFU ml^{-1}).[140] In this work, 50 nm gold-coated membrane filters were used to capture and aggregate bacteria directly from urine, while providing Raman signal enhancement for pathogen identification. The bacterial classification for the infected and uninfected urine samples was achieved with 91.1% accuracy. The assay was rapid and uncomplicated. However, the positive samples were constrained to three reference strain bacteria at a set concentration. Therefore, as per the previous assay, a larger number of reference bacterial species of varying strains and concentrations is required to be included in the chemometric training set to improve the diagnostic accuracy of the method. Additionally, a dual filtration is initially required to remove human sediments from urine prior to pathogen capture on SERS-active filters.

In another application, SERS was used for the discrimination between *E. faecalis* and *Streptococcus pyogenes* as Gram-positive bacteria demonstrators and other Gram-negative bacteria (*A. baumannii* and *K. pneumonia*).[141] The method reported the use of reproducible SERS substrate based on the re-crystallization of AgNPs in solution. First, AgNPs solution (28 nm) was mixed with 4M NaCl solution allowing their size to increase (~400 nm) and produce a higher SERS signal. Next, 0.05 mL of different bacterial cell lysates were added, incubated for 10 min and finally the Raman spectra were recorded. The obtained spectral datasets were subjected to a cluster analysis to identify each pathogen individually (Fig. 11). The cluster analysis was considered as an alternative way to identify the bacteria instead of evaluating particular peaks because it fully evaluated the whole spectral range. Therefore, it compared data between individual spectra more objectively while keeping the whole procedure as simple as possible. Compared to classical complicated histochemical methods that based on

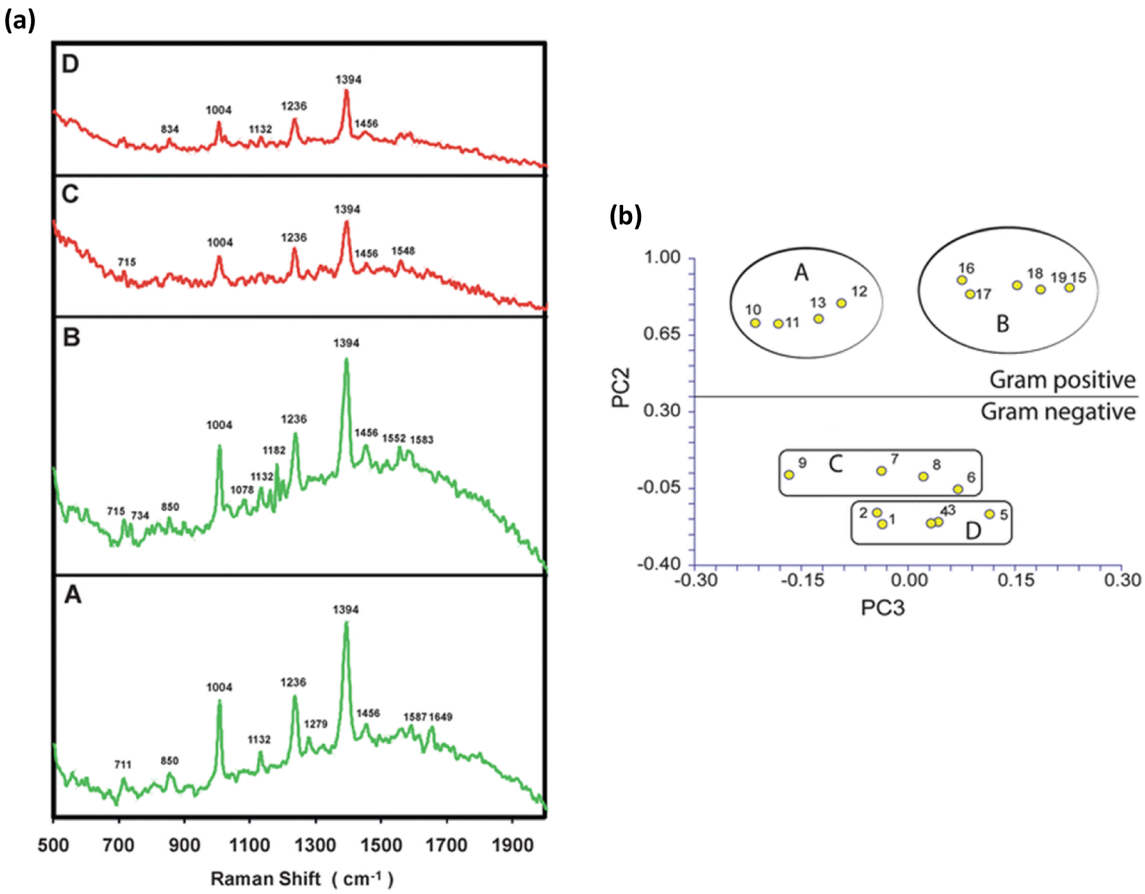

Fig. 11 (a) Representative SERS spectra of bacterial lysates: (A) *E. faecalis*, (B) *Streptococcus pyogenes*, (C) *Acinetobacter baumannii*, and (D) *K. pneumoniae*. (b) Cluster analysis of given Gram-positive and Gram-negative bacteria. The images are reprinted from Prucek *et al.*,[141] Copyright (2012), with permission from Royal Society of Chemistry.

staining a previously grown bacterial population, the reported method was robust, rapid (15 min) and easy to use.

A recent work by Zhou *et al.* demonstrated a novel proof-of-concept multifunctional nanocomplex that not only can be used for sensitive SERS detection of bacteria, but also have a bactericidal activity toward *VRE*.[142] In this work, silicon 2,3-naphthalocyanine dihydroxide (Nc) and vancomycin (Van) functionalised silica encapsulated, silver-coated AuNPs (Au@AgNP@SiO_2@Nc-Van) were developed as a novel theranostic system for the SERS detection and antimicrobial photodynamic therapy (aPDT) of *VRE* strains. The silver coated AuNPs acted as the SERS active platform producing strong SERS signal. Van enhanced the specific binding affinity toward *VRE* which was confirmed *via in vitro* bacterial SERS imaging. Si(IV) naphthalocyanine, that linked to the nanoparticle surface, served as a NIR photosensitizer that could photo inactivate the *VRE* upon NIR irradiation. The results revealed that a nanomolar concentration of the nanocomplex was sufficient to almost reduce 4–5 logs of *VRE* species. Furthermore, this hybrid nanomaterial was applied for the *in vivo* evaluation of *E. faecalis* lethality in mouse, resulting in fast and significant decrease in the infection compared to the non-treated group (Fig. 12). Compared to a previously reported conjugate,[143] this hybrid theranostic nanocomplex demonstrated better performance, in terms of biocompatibility, solubility, stability and complicated synthesis procedures. Additionally, the satisfactory SERS signals generated by the Au@AgNP core could serve as a promising alternative approach for fluorescence bacterial labelling. Importantly, the high *in vitro* aPDT effectiveness also could be translated into *in vivo* antimicrobial therapy, resulting in fast bacterial regression and even complete eradication. Although cytotoxicity and phototoxicity of NP@Nc-Van were examined in the HaCaT cell line using MTT assay, comprehensive *in vivo* studies should be performed and validated to exclusively tackle the toxicity issues related to nanoparticles on human health.

The SERS detection of the other main *VRE* pathogen, *E. faecium*, was reported by Qiu *et al.*[144] In this method, a one-

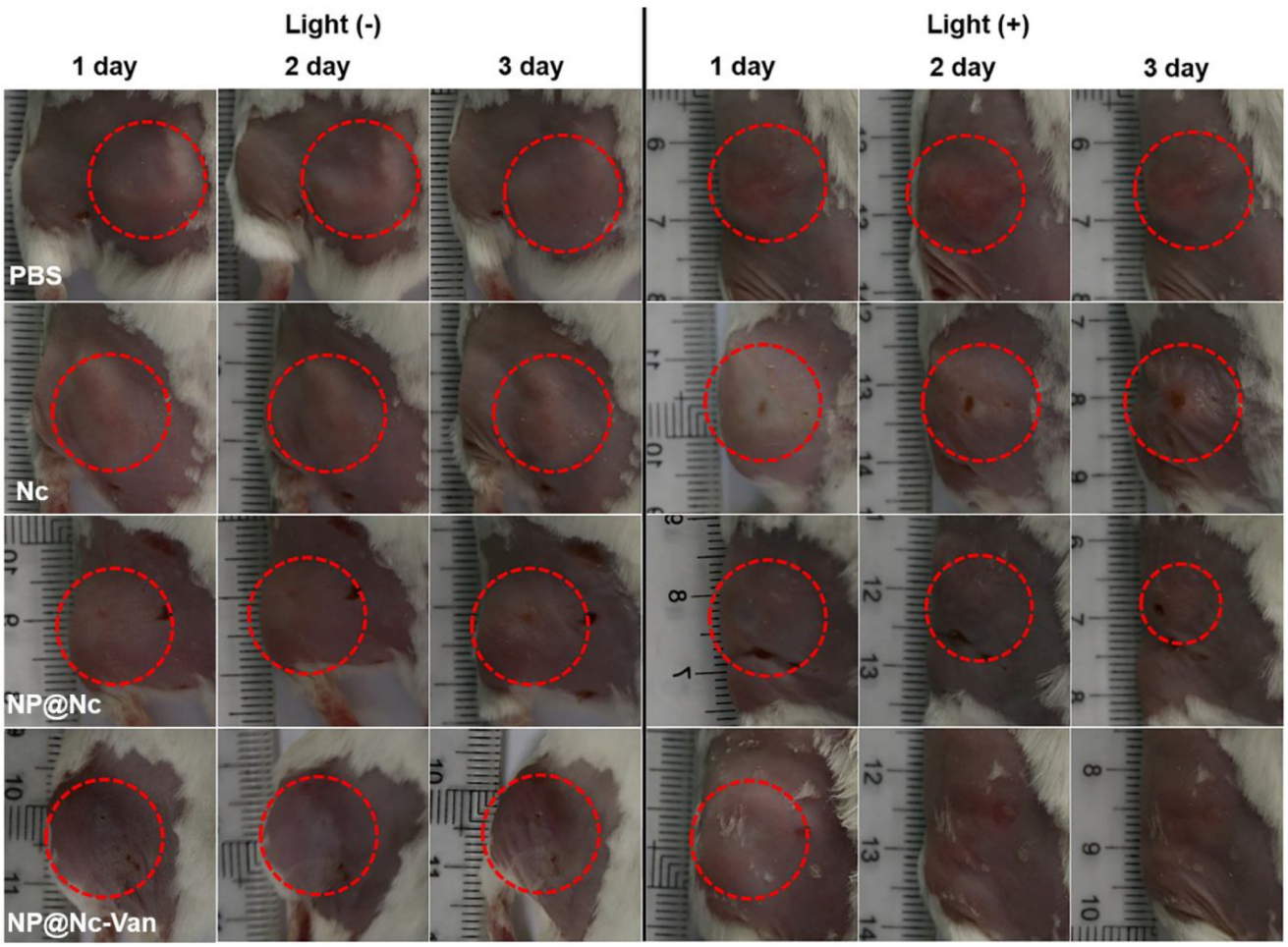

Fig. 12 *In vivo* photodynamic therapy of mice with *E. faecalis* infected wounds. Color photographs of infection sites (wounds created at the hindlimbs of the mice) from different experimental groups (PBS-treated groups, Nc groups, NP@Nc and NP@Nc-Van groups with or without illumination). NP@Nc-Van with illumination showed the highest antibacterial capability and fastest infection regression compared with those in other three groups. An obvious abscess was still observed in the dark group. The image is reprinted from Zhou *et al.*,[142] Copyright (2018), with permission from Elsevier.

step assembling and SERS sensing strategy was developed for the detection of three Gram-positive bacteria (*Staphylococcus xylosus*, *Listeria monocytogenes* and *E. faecium*). A positively charged columnar array of Au@Ag nanorods was designed as a large-scale uniform highly sensitive SERS substrate. Additionally, a plasmonic superstructure bifacial assembly of triangular gold nanoplates-gold nanospheres (TAuNPs-AuNSs) was synthesised to provide plenty of optical hotspots for further SERS enhancement. As Gram-positive bacteria has a high negative charge due to peptidoglycan of the cell wall, electrostatic interaction between bacteria and the functionalized nanorod columnar array was achieved resulting in efficient accumulation of bacteria onto the substrate surface. Later, the highly positively charged TAuNP-AuNSs superstructures were adsorbed onto the substrate surface-containing bacteria through the strong electrostatic interaction. Thus, the negatively-charged bacteria were efficiently trapped within the TAuNPs-AuNSs superstructures on top of the columnar array of Au@Ag nanorods. The SERS spectra collection was started when shrinking of the liquid droplet was recorded. The resultant spectra of the three bacteria were identical. Therefore, 3D PCA chemometric analysis was used to enable a highly sensitive mono species detection and mixed species discrimination. Additionally, the ratio of different bacteria was determined by aid of the chemometric analysis on the basis of the clustered SERS spectra. The reported plasmonic design enabled a rapid and highly sensitive detection for the three bacterial species with LOD of 50, 100, and 100 CFU mL^{-1}, respectively.

In another recent study, organometal-based SERS method using EC deposition onto plasmonic metal nanopillars Au substrate (MPs) combined with complementary DNAs (cDNAs) was described for the detection of *E. faecium* and *S. aureus*.[145] In this method, capture DNAs were designed with target-specific sequences to the pathogenic bacteria and attached to the MPs surface. A Raman dye cyanine 5 was attached to a probe DNAs for EC-SERS detection. By applying a redox potential, active hotspot engineering onto MPs-cDNAs was produced through *in situ* EC deposition of Au layer onto MPs-cDNAs within a short time (<10 min) and simultaneously produced SERS signals. The electric field confined in cDNAs surrounded by Au greatly amplifies the SERS signal of the Raman dye. The reported LOD was ~0.035 nM. The platform was also used to detect 0.1 nM bacterial DNAs in human whole blood sample.

4.5. *Neisseria gonorrhoea* (*NG*)

Patients with *NG* infection are often asymptomatic or may experience different symptoms that are not specific for gonorrhoea. This can result in uncertain diagnosis for the infection until complications arise, such as: pelvic inflammatory disease, ectopic pregnancy, infertility and disseminated gonococcal infection where *NG* spreads to the blood or other parts of the body.[11] Therefore, timely, accurate and sensitive testing is required for the early detection of *NG* infection to reduce the transmission of infection. The traditional culture methods for *NG* detection are sensitive and specific. However, they are very slow due to the elongated time required for laboratory cultured growth (≥48 hours) which make it impractical for POC testing.[11] NAAT-based methods are growth-free offering fast results with reasonable sensitivity and specificity. However, the significantly reduced assay time of SERS-based methods and the simplified procedure while maintaining a high sensitivity make SERS highly competitive with complex NAAT procedure currently applied for the clinical diagnosis of *NG* and other sexually transmitted diseases (STDs).

Chen *et al.* reported a SERS method for the rapid (<1 hour) and low-cost detection of *Chlamydia trachomatis* and *NG*.[11] In this method, AuNPs and AgNPs covered SiO_2 substrates were developed by a metal ion doped sol–gel, leading to the formation of small aggregates of monodispersed AuNPs and AgNPs (~80–100 nm) covering the outer layer of ~1 mm^2 SiO_2 surface. These substrates were then used to acquire the SERS signal of enriched bacterial cellular suspensions. Although both species are Gram-negative bacteria, their SERS spectra were completely different. The unique SERS signatures on Au and Ag substrates distinguished between these two bacteria and was the basis for the identification methodology. The reported SERS diagnostics sensitivity were 10^2–10^4 IFU mL^{-1} and 10^5 CFU mL^{-1} for *Chlamydia trachomatis* and *NG*, respectively. The SERS spectra of the cell-free supernatant surrounding both bacterial cells were also obtained by the Au and Ag substrates for the monitoring of the bacteria metabolic and enzymatic activity. Therefore, this label and growth-free method demonstrated the potential of SERS to be a sensitive and real-time bioanalytical tool for studying the bacterial biochemical activity in cell wall and extracellular regions. Thus, providing a better treatment efficacy and disease prognosis than NAATs.

In a very recent study, Berus *et al.*[146] reported a rapid (<15 min), sensitive (10^2 CFU mL^{-1}) and comprehensive SERS-chemometric analysis of *NG* in men's urethra swabs with another four bacterial pathogens, all being responsible for STDs, using silicon-based SERS substrates sputtered with 100 nm Ag layer. The method discussed the STD diagnosis in a direct and indirect manner, where the indirect (confirmatory) approach identified the unknown pathogenic strains in the clinical samples through matching their spectral images to other spectral images of different bacteria. While the direct one classified the SERS spectra of clinical samples to the correct group by using chemometric models. The method demonstrated successful differentiation of *NG* from the other four bacterial species with a 77% accuracy using PCA. Additionally, it demonstrated the differentiation of *NG* from other *Neisseria* strains with an accuracy of 92.5 ± 0.5%. The use of both non-supervised model (PCA) and supervised models (PLS1-DA), soft independent modelling of class analogies (SIMCA) allowed for the characterization, differentiation and classification of clinical samples with a prediction accuracy reaching 100% for PLS1-DA and 89% for SIMCA. Therefore, the proposed SERS-based sensor combined with the appropriate chemometric models can be applied for the uncomplicated and fast discrimination between infected and uninfected urethra swabs.

5. Conclusion and future perspective

Antibiotic resistance poses a real and significant global threat to human health against a backdrop of an antibiotics supply pipeline which is drying up. This critical problem requires global solutions and initiatives, such as raising awareness of antibiotic resistance, better surveillance and improved antibiotic dosing regimens. More importantly, the implementation of rapid, sensitive, and point-of-care diagnostic tests that can correctly identify pathogenic bacteria and any associated resistance mechanisms. This will empower clinicians to decide if antibiotics are an appropriate treatment in the first instance, and if so, which antibiotic should be used based on the resistance information derived from the test.

In this review, we discussed the use of SERS as a powerful alternative diagnostic technique that can be used for the ultra-sensitive, rapid, and accurate detection of bacterial infection instead of traditional culture-based and NAATs methods. Additionally, we pointed out the usefulness of SERS in the identification of the resistant and sensitive bacterial strains, as well as in the determination of antibiotic susceptibility of the bacteria. We also highlighted the recent SERS advances for the diagnosis of the "*Big 5*" antibiotic resistance challenges according to DALYs measure.

SERS demonstrated a strong capability for the real-time detection of bacterial pathogens and for the fundamental understanding of bacterial antibiotic resistance mechanisms. The fingerprint merit of the technique enabled SERS to be an excellent diagnostic tool for the identification of resistance biomarkers and for the susceptibility testing to indicate bacterial resistance to antibiotics. Despite SERS being applied successfully on multiple proof-of-concept bacterial diagnostics, there is now a need to optimize the level of standardization between laboratories to ensure repeatability and reproducibility of results to achieve significant clinical impact. Moreover, to take bacterial SERS diagnosis beyond the concept phase, defined validated standardized reference libraries that have been tested on large sample numbers are mandatory for all the bacteria that could be the causative form of an infection in different real-life complex matrices.

In the future, we believe that more efforts should be carried out to further combine SERS detection of pathogens with other resistance biomarkers identification tests and/or susceptibility testing. With the aid of standardized algorithms/chemometric models for SERS spectral analysis, the sample could be split and processed in parallel to generate two important pieces of information simultaneously in one sensitive, simple, and quick test. Furthermore, the future advance in instrumentation design and machine learning is expected to make SERS more user-friendly and cost-effective technique. Therefore, it can be used to a greater extent for the understanding of antibiotic resistance modes of the bacteria, which in turn will contribute efficiently towards the design of new effective antibiotics.

Author contributions

The manuscript was written through contributions of all authors and all authors have given approval to the final version of the manuscript.

Conflicts of interest

There are no conflicts to declare.

Acknowledgements

This work was supported by the EPSRC IRC in Early-Warning Sensing Systems for Infectious Diseases (i-sense) EP/K031953/1, EPSRC IRC in Agile Early Warning Sensing Systems for Infectious Diseases & Antimicrobial Resistance EP/R00529X/1 and IRC Next Steps Plus: Ultra-Sensitive Enhanced NanoSensing of Anti-Microbial Resistance (uSense) EP/R018391/1. The authors acknowledge the American Chemical Society, Elsevier, Royal Society of Chemistry, Springer and Springer Nature publication groups for the reprints of figures used in this review. For the purpose of open access, the author has applied a Creative Commons Attribution (CC BY) licence to any Author Accepted Manuscript version arising from this submission.

References

1 N. Sabtu, D. A. Enoch and N. M. Brown, *Br. Med. Bull.*, 2015, **116**, 105–113.
2 G. D. Kaprou, I. Bergšpica, E. A. Alexa, A. Alvarez-Ordóñez and M. Prieto, *Antibiotics*, 2021, **10**, 209.
3 R. E. Nelson, K. M. Hatfield, H. Wolford, M. H. Samore, R. D. Scott II, S. C. Reddy, B. Olubajo, P. Paul, J. A. Jernigan and J. Baggs, *Clin. Infect. Dis.*, 2021, **72**, S17–S26.
4 A. Cassini, L. D. Högberg, D. Plachouras, A. Quattrocchi, A. Hoxha, G. S. Simonsen, M. Colomb-Cotinat, M. E. Kretzschmar, B. Devleesschauwer, M. Cecchini, D. A. Ouakrim, T. C. Oliveira, M. J. Struelens, C. Suetens and D. L. Monnet, *Lancet Infect. Dis.*, 2019, **19**, 56–66.
5 A. Cassini, E. Colzani, A. Pini, M. J. Mangen, D. Plass, S. A. McDonald, G. Maringhini, A. van Lier, J. A. Haagsma, A. H. Havelaar, P. Kramarz and M. E. Kretzschmar, *Eurosurveillance*, 2018, **23**, 17–00454.
6 T. Wi, M. M. Lahra, F. Ndowa, M. Bala, J. R. Dillon, P. Ramon-Pardo, S. R. Eremin, G. Bolan and M. Unemo, *PLoS Med.*, 2017, **14**, e1002344.
7 J. W.-F. Law, N.-S. Ab Mutalib, K.-G. Chan and L.-H. Lee, *Front. Microbiol.*, 2015, **5**, 770.
8 A. S. Chitnis, J. L. Davis, G. F. Schecter, P. M. Barry and J. M. Flood, *Infect. Control Hosp. Epidemiol.*, 2015, **36**, 1215–1225.
9 N. Singhal, M. Kumar, P. K. Kanaujia and J. S. Virdi, *Front. Microbiol.*, 2015, **6**, 791.

10 J. Leva-Bueno, S. A. Peyman and P. A. Millner, *Med. Microbiol. Immunol.*, 2020, **209**, 343–362.
11 Y. Chen, W. R. Premasiri and L. D. Ziegler, *Sci. Rep.*, 2018, **8**, 5163.
12 S. Sauer and M. Kliem, *Nat. Rev. Microbiol.*, 2010, **8**, 74–82.
13 L. A. Lawton and C. Edwards, *J. Chromatogr. A*, 2001, **912**, 191–209.
14 S. Sakamoto, W. Putalun, S. Vimolmangkang, W. Phoolcharoen, Y. Shoyama, H. Tanaka and S. Morimoto, *J. Nat. Med.*, 2018, **72**, 32–42.
15 L. Rassaei, F. Marken, M. Sillanpää, M. Amiri, C. M. Cirtiu and M. Sillanpää, *TrAC, Trends Anal. Chem.*, 2011, **30**, 1704–1715.
16 A. Chen and S. Chatterjee, *Chem. Soc. Rev.*, 2013, **42**, 5425–5438.
17 W. A. Hassanain, A. Sivanesan, G. A. Ayoko and E. L. Izake, *J. Electrochem. Soc.*, 2020, **167**, 067518.
18 M. Amiri, A. Bezaatpour, H. Jafari, R. Boukherroub and S. Szunerits, *ACS Sens.*, 2018, **3**, 1069–1086.
19 J. Docherty, S. Mabbott, E. Smith, K. Faulds, C. Davidson, J. Reglinski and D. Graham, *Analyst*, 2016, **141**, 5857–5863.
20 H. Kearns, R. Goodacre, L. E. Jamieson, D. Graham and K. Faulds, *Anal. Chem.*, 2017, **89**, 12666–12673.
21 B. Liu, P. Zhou, X. Liu, X. Sun, H. Li and M. Lin, *Food Bioprocess Technol.*, 2013, **6**, 710–718.
22 A. Subaihi, L. Almanqur, H. Muhamadali, N. AlMasoud, D. I. Ellis, D. K. Trivedi, K. A. Hollywood, Y. Xu and R. Goodacre, *Anal. Chem.*, 2016, **88**, 10884–10892.
23 W. A. Hassanain, J. Spoors, C. L. Johnson, K. Faulds, N. Keegan and D. Graham, *Analyst*, 2021, **146**, 4495–4505.
24 S. Laing, K. Gracie and K. Faulds, *Chem. Soc. Rev.*, 2016, **45**, 1901–1918.
25 D. Graham, M. Moskovits and Z.-Q. Tian, *Chem. Soc. Rev.*, 2017, **46**, 3864–3865.
26 J. S. Bartlett, K. J. Voss, S. Sathyendranath and A. Vodacek, *Appl. Opt.*, 1998, **37**, 3324–3332.
27 L. E. Jamieson, S. M. Asiala, K. Gracie, K. Faulds and D. Graham, *Annu. Rev. Anal. Chem.*, 2017, **10**, 415–437.
28 K. C. Bantz, A. F. Meyer, N. J. Wittenberg, H. Im, Ö. Kurtuluş, S. H. Lee, N. C. Lindquist, S.-H. Oh and C. L. Haynes, *Phys. Chem. Chem. Phys.*, 2011, **13**, 11551–11567.
29 F. Shan, X.-Y. Zhang, X.-C. Fu, L.-J. Zhang, D. Su, S.-J. Wang, J.-Y. Wu and T. Zhang, *Sci. Rep.*, 2017, **7**, 6813.
30 K. Gracie, E. Correa, S. Mabbott, J. A. Dougan, D. Graham, R. Goodacre and K. Faulds, *Chem. Sci.*, 2014, **5**, 1030–1040.
31 W. Gao, B. Li, R. Yao, Z. Li, X. Wang, X. Dong, H. Qu, Q. Li, N. Li, H. Chi, B. Zhou and Z. Xia, *Anal. Chem.*, 2017, **89**, 9836–9842.
32 A. Subaihi, D. K. Trivedi, K. A. Hollywood, J. Bluett, Y. Xu, H. Muhamadali, D. I. Ellis and R. Goodacre, *Anal. Chem.*, 2017, **89**, 6702–6709.
33 W. A. Hassanain, E. L. Izake, A. Sivanesan and G. A. Ayoko, *J. Pharm. Biomed. Anal.*, 2017, **136**, 38–43.
34 V. Peksa, P. Lebrušková, H. Šípová, J. Štěpánek, J. Bok, J. Homola and M. Procházka, *Phys. Chem. Chem. Phys.*, 2016, **18**, 19613–19620.
35 J. Langer, D. Jimenez de Aberasturi, J. Aizpurua, R. A. Alvarez-Puebla, B. Auguié, J. J. Baumberg, G. C. Bazan, S. E. J. Bell, A. Boisen, A. G. Brolo, J. Choo, D. Cialla-May, V. Deckert, L. Fabris, K. Faulds, F. J. García de Abajo, R. Goodacre, D. Graham, A. J. Haes, C. L. Haynes, C. Huck, T. Itoh, M. Käll, J. Kneipp, N. A. Kotov, H. Kuang, E. C. Le Ru, H. K. Lee, J.-F. Li, X. Y. Ling, S. A. Maier, T. Mayerhöfer, M. Moskovits, K. Murakoshi, J.-M. Nam, S. Nie, Y. Ozaki, I. Pastoriza-Santos, J. Perez-Juste, J. Popp, A. Pucci, S. Reich, B. Ren, G. C. Schatz, T. Shegai, S. Schlücker, L.-L. Tay, K. G. Thomas, Z.-Q. Tian, R. P. Van Duyne, T. Vo-Dinh, Y. Wang, K. A. Willets, C. Xu, H. Xu, Y. Xu, Y. S. Yamamoto, B. Zhao and L. M. Liz-Marzán, *ACS Nano*, 2020, **14**, 28–117.
36 S. Fornasaro, F. Alsamad, M. Baia, L. A. E. Batista de Carvalho, C. Beleites, H. J. Byrne, A. Chiadò, M. Chis, M. Chisanga, A. Daniel, J. Dybas, G. Eppe, G. Falgayrac, K. Faulds, H. Gebavi, F. Giorgis, R. Goodacre, D. Graham, P. La Manna, S. Laing, L. Litti, F. M. Lyng, K. Malek, C. Malherbe, M. P. M. Marques, M. Meneghetti, E. Mitri, V. Mohaček-Grošev, C. Morasso, H. Muhamadali, P. Musto, C. Novara, M. Pannico, G. Penel, O. Piot, T. Rindzevicius, E. A. Rusu, M. S. Schmidt, V. Sergo, G. D. Sockalingum, V. Untereiner, R. Vanna, E. Wiercigroch and A. Bonifacio, *Anal. Chem.*, 2020, **92**, 4053–4064.
37 S. E. J. Bell, G. Charron, E. Cortés, J. Kneipp, M. L. de la Chapelle, J. Langer, M. Procházka, V. Tran and S. Schlücker, *Angew. Chem., Int. Ed.*, 2020, **59**, 5454–5462.
38 Y. Liu, H. Zhou, Z. Hu, G. Yu, D. Yang and J. Zhao, *Biosens. Bioelectron.*, 2017, **94**, 131–140.
39 M. Fleischmann, P. J. Hendra and A. J. McQuillan, *Chem. Phys. Lett.*, 1974, **26**, 163–166.
40 D. L. Jeanmaire and R. P. Van Duyne, *J. Electroanal. Chem. Interfacial Electrochem.*, 1977, **84**, 1–20.
41 M. Chisanga, H. Muhamadali, D. I. Ellis and R. Goodacre, *Appl. Sci.*, 2019, **9**, 1163.
42 H.-n. Xie, I. A. Larmour, W. E. Smith, K. Faulds and D. Graham, *Analyst*, 2012, **137**, 2297–2299.
43 K. Wang, S. Li, M. Petersen, S. Wang and X. Lu, *Nanomaterials*, 2018, **8**, 762.
44 Y. Wang and J. Irudayaraj, *Philos. Trans. R. Soc., B*, 2013, **368**, 20120026.
45 L. Hamm, A. Gee and A. S. D. S. Indrasekara, *Appl. Sci.*, 2019, **9**, 1448.
46 A. X. Wang and X. Kong, *Materials*, 2015, **8**, 3024–3052.
47 M. R. Jones, K. D. Osberg, R. J. Macfarlane, M. R. Langille and C. A. Mirkin, *Chem. Rev.*, 2011, **111**, 3736–3827.
48 N. G. Bastús, J. Comenge and V. Puntes, *Langmuir*, 2011, **27**, 11098–11105.
49 S. Neretina, R. A. Hughes, K. D. Gilroy and M. Hajfathalian, *Acc. Chem. Res.*, 2016, **49**, 2243–2250.

50 X. Yang, M. Yang, B. Pang, M. Vara and Y. Xia, *Chem. Rev.*, 2015, **115**, 10410–10488.
51 L. Guerrini, Ž. Krpetić, D. van Lierop, R. A. Alvarez-Puebla and D. Graham, *Angew. Chem., Int. Ed.*, 2015, **54**, 1144–1148.
52 H. Zhou, D. Yang, N. P. Ivleva, N. E. Mircescu, R. Niessner and C. Haisch, *Anal. Chem.*, 2014, **86**, 1525–1533.
53 M. Kahraman, A. I. Zamaleeva, R. F. Fakhrullin and M. Culha, *Anal. Bioanal. Chem.*, 2009, **395**, 2559–2567.
54 L. Guerrini and D. Graham, *Chem. Soc. Rev.*, 2012, **41**, 7085–7107.
55 M. Fan, G. F. S. Andrade and A. G. Brolo, *Anal. Chim. Acta*, 2011, **693**, 7–25.
56 Z. Fan, R. Kanchanapally and P. C. Ray, *J. Phys. Chem. Lett.*, 2013, **4**, 3813–3818.
57 S. Jones, A. Pramanik, R. Kanchanapally, B. P. V. Nellore, S. Begum, C. Sweet and P. C. Ray, *ACS Sustainable Chem. Eng.*, 2017, **5**, 7175–7187.
58 X. Xie, H. Pu and D.-W. Sun, *Crit. Rev. Food Sci. Nutr.*, 2018, **58**, 2800–2813.
59 X. Wu, C. Xu, R. A. Tripp, Y.-w. Huang and Y. Zhao, *Analyst*, 2013, **138**, 3005–3012.
60 Z. Wang, S. Zong, L. Wu, D. Zhu and Y. Cui, *Chem. Rev.*, 2017, **117**, 7910–7963.
61 C. Zong, M. Xu, L.-J. Xu, T. Wei, X. Ma, X.-S. Zheng, R. Hu and B. Ren, *Chem. Rev.*, 2018, **118**, 4946–4980.
62 W. A. Hassanain, E. L. Izake, M. S. Schmidt and G. A. Ayoko, *Biosens. Bioelectron.*, 2017, **91**, 664–672.
63 D. Yang, H. Zhou, C. Haisch, R. Niessner and Y. Ying, *Talanta*, 2016, **146**, 457–463.
64 N. Duan, B. Chang, H. Zhang, Z. Wang and S. Wu, *Int. J. Food Microbiol.*, 2016, **218**, 38–43.
65 D. D. Galvan and Q. Yu, *Adv. Healthcare Mater.*, 2018, **7**, 1701335.
66 H. Zhou, D. Yang, N. P. Ivleva, N. E. Mircescu, S. Schubert, R. Niessner, A. Wieser and C. Haisch, *Anal. Chem.*, 2015, **87**, 6553–6561.
67 H. Wang, Y. Zhou, X. Jiang, B. Sun, Y. Zhu, H. Wang, Y. Su and Y. He, *Angew. Chem., Int. Ed.*, 2015, **54**, 5132–5136.
68 P. Wang, S. Pang, J. Chen, L. McLandsborough, S. R. Nugen, M. Fan and L. He, *Analyst*, 2016, **141**, 1356–1362.
69 H. Marks, M. Schechinger, J. Garza, A. Locke and G. Coté, *Nanophotonics*, 2017, **6**, 681.
70 R. Wang, K. Kim, N. Choi, X. Wang, J. Lee, J. H. Jeon, G.-e. Rhie and J. Choo, *Sens. Actuators, B*, 2018, **270**, 72–79.
71 J. Hwang, S. Lee and J. Choo, *Nanoscale*, 2016, **8**, 11418–11425.
72 S. H. Lee, J. Hwang, K. Kim, J. Jeon, S. Lee, J. Ko, J. Lee, M. Kang, D. R. Chung and J. Choo, *Anal. Chem.*, 2019, **91**, 12275–12282.
73 C. Catala, B. Mir-Simon, X. Feng, C. Cardozo, N. Pazos-Perez, E. Pazos, S. Gómez-de Pedro, L. Guerrini, A. Soriano, J. Vila, F. Marco, E. Garcia-Rico and R. A. Alvarez-Puebla, *Adv. Mater. Technol.*, 2016, **1**, 1600163.
74 Y. Wang, S. Rauf, Y. S. Grewal, L. J. Spadafora, M. J. A. Shiddiky, G. A. Cangelosi, S. Schlücker and M. Trau, *Anal. Chem.*, 2014, **86**, 9930–9938.
75 I. F. Cheng, H.-C. Chang, T.-Y. Chen, C. Hu and F.-L. Yang, *Sci. Rep.*, 2013, **3**, 2365–2365.
76 H.-Y. Lin, C.-H. Huang, W.-H. Hsieh, L.-H. Liu, Y.-C. Lin, C.-C. Chu, S.-T. Wang, I.-T. Kuo, L.-K. Chau and C.-Y. Yang, *Small*, 2014, **10**, 4700–4710.
77 A. Vasala, V. P. Hytönen and O. H. Laitinen, *Front. Cell. Infect. Microbiol.*, 2020, **10**, 308.
78 Y. Cheong, Y. J. Kim, H. Kang, S. Choi and H. J. Lee, *Spectrochim. Acta, Part A*, 2017, **183**, 53–59.
79 X. Lu, D. R. Samuelson, Y. Xu, H. Zhang, S. Wang, B. A. Rasco, J. Xu and M. E. Konkel, *Anal. Chem.*, 2013, **85**, 2320–2327.
80 A. Mühlig, T. Bocklitz, I. Labugger, S. Dees, S. Henk, E. Richter, S. Andres, M. Merker, S. Stöckel, K. Weber, D. Cialla-May and J. Popp, *Anal. Chem.*, 2016, **88**, 7998–8004.
81 N. E. Mircescu, H. Zhou, N. Leopold, V. Chiș, N. P. Ivleva, R. Niessner, A. Wieser and C. Haisch, *Anal. Bioanal. Chem.*, 2014, **406**, 3051–3058.
82 T.-Y. Liu, K.-T. Tsai, H.-H. Wang, Y. Chen, Y.-H. Chen, Y.-C. Chao, H.-H. Chang, C.-H. Lin, J.-K. Wang and Y.-L. Wang, *Nat. Commun.*, 2011, **2**, 538.
83 H.-K. Huang, H.-W. Cheng, C.-C. Liao, S.-J. Lin, Y.-Z. Chen, J.-K. Wang, Y.-L. Wang and N.-T. Huang, *Lab Chip*, 2020, **20**, 2520–2528.
84 K.-W. Chang, H.-W. Cheng, J. Shiue, J.-K. Wang, Y.-L. Wang and N.-T. Huang, *Anal. Chem.*, 2019, **91**, 10988–10995.
85 S.-J. Lin, P.-H. Chao, H.-W. Cheng, J.-K. Wang, Y.-L. Wang, Y.-Y. Han and N.-T. Huang, *Lab Chip*, 2022, **22**, 1805–1814.
86 O. Samek, S. Bernatová and F. Dohnal, *Nanophotonics*, 2021, **10**, 2537–2561.
87 T.-T. Liu, Y.-H. Lin, C.-S. Hung, T.-J. Liu, Y. Chen, Y.-C. Huang, T.-H. Tsai, H.-H. Wang, D.-W. Wang, J.-K. Wang, Y.-L. Wang and C.-H. Lin, *PLoS One*, 2009, **4**, e5470.
88 C.-Y. Liu, Y.-Y. Han, P.-H. Shih, W.-N. Lian, H.-H. Wang, C.-H. Lin, P.-R. Hsueh, J.-K. Wang and Y.-L. Wang, *Sci. Rep.*, 2016, **6**, 23375.
89 P. Wang, S. Pang, H. Zhang, M. Fan and L. He, *Anal. Bioanal. Chem.*, 2016, **408**, 933–941.
90 C.-C. Liao, Y.-Z. Chen, S.-J. Lin, H.-W. Cheng, J.-K. Wang, Y.-L. Wang, Y.-Y. Han and N.-T. Huang, *Biosens. Bioelectron.*, 2021, **191**, 113483.
91 W. J. Thrift, S. Ronaghi, M. Samad, H. Wei, D. G. Nguyen, A. S. Cabuslay, C. E. Groome, P. J. Santiago, P. Baldi, A. I. Hochbaum and R. Ragan, *ACS Nano*, 2020, **14**, 15336–15348.
92 N. A. Turner, B. K. Sharma-Kuinkel, S. A. Maskarinec, E. M. Eichenberger, P. P. Shah, M. Carugati, T. L. Holland and V. G. Fowler, *Nat. Rev. Microbiol.*, 2019, **17**, 203–218.
93 Z. Zhang, X. Han, Z. Wang, Z. Yang, W. Zhang, J. Li, H. Yang, X. Y. Ling and B. Xing, *Chem. Commun.*, 2018, **54**, 7022–7025.

94 P. R. Potluri, V. K. Rajendran, A. Sunna and Y. Wang, *Analyst*, 2020, **145**, 2789–2794.
95 S. M. Restaino and I. M. White, *Lab Chip*, 2018, **18**, 832–839.
96 L. Chen, N. Mungroo, L. Daikuara and S. Neethirajan, *J. Nanobiotechnol.*, 2015, **13**, 45.
97 C. Wang, B. Gu, Q. Liu, Y. Pang, R. Xiao and S. Wang, *Int. J. Nanomed.*, 2018, **13**, 1159–1178.
98 S. Wang, H. Dong, W. Shen, Y. Yang, Z. Li, Y. Liu, C. Wang, B. Gu and L. Zhang, *RSC Adv.*, 2021, **11**, 34425–34431.
99 F. U. Ciloglu, A. M. Saridag, I. H. Kilic, M. Tokmakci, M. Kahraman and O. Aydin, *Analyst*, 2020, **145**, 7559–7570.
100 F. U. Ciloglu, A. Caliskan, A. M. Saridag, I. H. Kilic, M. Tokmakci, M. Kahraman and O. Aydin, *Sci. Rep.*, 2021, **11**, 18444.
101 J. He, Y. Qiao, H. Zhang, J. Zhao, W. Li, T. Xie, D. Zhong, Q. Wei, S. Hua, Y. Yu, K. Yao, H. A. Santos and M. Zhou, *Biomaterials*, 2020, **234**, 119763.
102 S. Xiang, Y. Lan, Z. Mai, F. Tian and H. Mao, *Spectrochim. Acta, Part A*, 2022, 121611.
103 Z. Breijyeh, B. Jubeh and R. Karaman, *Molecules*, 2020, **25**, 1340.
104 H. Wilson and M. E. Török, *Microb. Genomics*, 2018, **4**, e000197.
105 D. Willemse-Erix, T. Bakker-Schut, F. Slagboom-Bax, J.-w. Jachtenberg, N. Lemmens-den Toom, C. C. Papagiannitsis, K. Kuntaman, G. Puppels, A. van Belkum, J. A. Severin, W. Goessens and K. Maquelin, *J. Clin. Microbiol.*, 2012, **50**, 1370–1375.
106 S. Telhig, L. Ben Said, S. Zirah, I. Fliss and S. Rebuffat, *Front. Microbiol.*, 2020, **11**, 586433.
107 C. N. Kotanen, L. Martinez, R. Alvarez and J. W. Simecek, *Sens. Bio-Sens. Res.*, 2016, **8**, 20–26.
108 C.-C. Lin, C.-Y. Lin, C.-J. Kao and C.-H. Hung, *Sens. Actuators, B*, 2017, **241**, 513–521.
109 W. Liu, J. W. Tang, J. W. Lyu, J. J. Wang, Y. C. Pan, X. Y. Shi, Q. H. Liu, X. Zhang, B. Gu and L. Wang, *Microbiol. Spectrum*, 2022, **10**, e0240921.
110 S. Jones, S. S. Sinha, A. Pramanik and P. C. Ray, *Nanoscale*, 2016, **8**, 18301–18308.
111 Y. Wang, Q. Li, R. Zhang, K. Tang, C. Ding and S. Yu, *Microchim. Acta*, 2020, **187**, 290.
112 H. Yilmaz, S. S. Mohapatra and M. Culha, *Spectrochim. Acta, Part A*, 2022, **268**, 120699.
113 A. H. Arslan, F. U. Ciloglu, U. Yilmaz, E. Simsek and O. Aydin, *Spectrochim. Acta, Part A*, 2022, **267**, 120475.
114 Y. Li, F. Gao, C. Lu, M.-L. Fauconnier and J. Zheng, *Biosensors*, 2021, **11**, 354.
115 H.-b. Liu, C.-y. Chen, C.-n. Zhang, X.-j. Du, P. Li and S. Wang, *J. Food Sci.*, 2019, **84**, 2916–2924.
116 S. Asgari, R. Dhital, S. A. Aghvami, A. Mustapha, Y. Zhang and M. Lin, *Microchim. Acta*, 2022, **189**, 111.
117 Y. Yang, C. Zeng, J. Huang, M. Wang, W. Qi, H. Wang and Z. He, *Biosens. Bioelectron.*, 2022, **215**, 114524.
118 S.-M. You, K. Luo, J.-Y. Jung, K.-B. Jeong, E.-S. Lee, M.-H. Oh and Y.-R. Kim, *ACS Appl. Mater. Interfaces*, 2020, **12**, 18292–18300.
119 Y.-W. Weng, X.-D. Hu, L. Jiang, Q.-L. Shi and X.-L. Wei, *Anal. Bioanal. Chem.*, 2021, **413**, 5419–5426.
120 S. Díaz-Amaya, L.-K. Lin, A. J. Deering and L. A. Stanciu, *Anal. Chim. Acta*, 2019, **1081**, 146–156.
121 Y. L. Wong, W. C. M. Kang, M. Reyes, J. W. P. Teo and J. C. Y. Kah, *ACS Infect. Dis.*, 2020, **6**, 947–953.
122 S. H. Hilton, C. Hall, H. T. Nguyen, M. L. Everitt, P. DeShong and I. M. White, *Anal. Chim. Acta*, 2020, **1127**, 207–216.
123 Z. Li, L. Leustean, F. Inci, M. Zheng, U. Demirci and S. Wang, *Biotechnol. Adv.*, 2019, **37**, 107440.
124 S. Tabbasum, M. I. Majeed, H. Nawaz, N. Rashid, M. Tahira, A. Mohsin, A. Arif, A. u. Haq, M. Saleem, G. Dastgir, F. Batool and S. Bashir, *Photodiagn. Photodyn. Ther.*, 2021, **35**, 102426.
125 N. A. Owens, A. Pinter and M. D. Porter, *J. Raman Spectrosc.*, 2019, **50**, 15–25.
126 A. C. Crawford, L. B. Laurentius, T. S. Mulvihill, J. H. Granger, J. S. Spencer, D. Chatterjee, K. E. Hanson and M. D. Porter, *Analyst*, 2017, **142**, 186–196.
127 L. B. Laurentius, A. C. Crawford, T. S. Mulvihill, J. H. Granger, R. Robinson, J. S. Spencer, D. Chatterjee, K. E. Hanson and M. D. Porter, *Analyst*, 2017, **142**, 177–185.
128 N. A. Owens, L. B. Laurentius, M. D. Porter, Q. Li, S. Wang and D. Chatterjee, *Appl. Spectrosc.*, 2018, **72**, 1104–1115.
129 N. R. Hendricks-Leukes, M. R. Jonas, Z. C. Mlamla, M. Smith and J. M. Blackburn, *ACS Sens.*, 2022, **7**, 1403–1418.
130 R. A. Karaballi, A. Nel, S. Krishnan, J. Blackburn and C. L. Brosseau, *Phys. Chem. Chem. Phys.*, 2015, **17**, 21356–21363.
131 J. Perumal, U. S. Dinish, A. K. Bendt, A. Kazakeviciute, C. Y. Fu, I. L. H. Ong and M. Olivo, *Int. J. Nanomed.*, 2018, **13**, 6029–6038.
132 W.-C. Cheng, L.-H. Chen, C.-R. Jiang, Y.-M. Deng, D.-W. Wang, C.-H. Lin, R. Jou, J.-K. Wang and Y.-L. Wang, *Anal. Chem.*, 2021, **93**, 2785–2792.
133 R. Botta, P. Chindaudom, P. Eiamchai, M. Horprathum, S. Limwichean, C. Chananonnawathorn, V. Patthanasettakul, B. Kaewseekhao, K. Faksri and N. Nuntawong, *Tuberculosis*, 2018, **108**, 195–200.
134 B. Kaewseekhao, N. Nuntawong, P. Eiamchai, S. Roytrakul, W. Reechaipichitkul and K. Faksri, *Tuberculosis*, 2020, **121**, 101916.
135 J. Wang, Q. Chen, T. Belwal, X. Lin and Z. Luo, *Compr. Rev. Food Sci. Food Saf.*, 2021, **20**, 2476–2507.
136 H. S. Kafil and M. Asgharzadeh, *Maedica*, 2014, **9**, 323–327.
137 U. Ch. Schröder, C. Beleites, C. Assmann, U. Glaser, U. Hübner, W. Pfister, W. Fritzsche, J. Popp and U. Neugebauer, *Sci. Rep.*, 2015, **5**, 8217.

138 H. H. Shin, H. J. Lee, M. J. Hwang, J. Kim, H. Kim, S. H. Nam, J. S. Park, J. E. Hwang, E. S. Kim, Y. S. Park, Y. D. Suh and D.-K. Lim, *Sens. Actuators, B*, 2021, **349**, 130784.

139 N. Tien, T.-H. Lin, Z.-C. Hung, H.-S. Lin, I. K. Wang, H.-C. Chen and C.-T. Chang, *Molecules*, 2018, **23**, 3374.

140 S. D. Dryden, S. Anastasova, G. Satta, A. J. Thompson, D. R. Leff and A. Darzi, *Sci. Rep.*, 2021, **11**, 8802.

141 R. Prucek, V. Ranc, L. Kvítek, A. Panáček, R. Zbořil and M. Kolář, *Analyst*, 2012, **137**, 2866–2870.

142 Z. Zhou, S. Peng, M. Sui, S. Chen, L. Huang, H. Xu and T. Jiang, *Colloids Surf., B*, 2018, **161**, 394–402.

143 B. Xing, T. Jiang, W. Bi, Y. Yang, L. Li, M. Ma, C.-K. Chang, B. Xu and E. K. L. Yeow, *Chem. Commun.*, 2011, **47**, 1601–1603.

144 L. Qiu, W. Wang, A. Zhang, N. Zhang, T. Lemma, H. Ge, J. J. Toppari, V. P. Hytönen and J. Wang, *ACS Appl. Mater. Interfaces*, 2016, **8**, 24394–24403.

145 S. H. Lee, W.-C. Lee, E. H. Koh, I. B. Ansah, J.-Y. Yang, C. Mun, S. Lee, D.-H. Kim, H. S. Jung and S.-G. Park, *Biosens. Bioelectron.*, 2022, **210**, 114325.

146 S. M. Berus, M. Adamczyk-Popławska, B. Młynarczyk-Bonikowska, E. Witkowska, T. Szymborski, J. Waluk and A. Kamińska, *Biosens. Bioelectron.*, 2021, **189**, 113358.

